THERMALLY STIMULATED CURRENT STUDY OF TRAPS DISTRIBUTION IN TlGaSeS LAYERED SINGLE CRYSTALS

A THESIS SUBMITTED TO
THE GRADUATE SCHOOL OF NATURAL AND APPLIED SCIENCES
OF
MIDDLE EAST TECHNICAL UNIVERSITY

BY

HISHAM NASSER

IN PARTIAL FULFILMENT OF THE REQUIREMENTS
FOR
THE DEGREE OF MASTER OF SCIENCE
IN
PHYSICS

MAY 2010

Approval of the thesis:

THERMALLY STIMULATED CURRENT STUDY OF TRAPS DISTRIBUTION IN TlGaSeS LAYERED SINGLE CRYSTALS

submitted by **HISHAM NASSER** in partial fulfilment of the requirements for the degree of **Master of Science in Physics Department, Middle East Technical University** by,

Prof. Dr. Canan Özgen
Dean, Graduate School of **Natural and Applied Sciences** _________________

Prof. Dr. Sinan Bilikmen
Head of the Department, **Physics** _________________

Prof. Dr. Nizami Hasanli
Supervisor, **Physics Dept., METU** _________________

Examining Committee Members:

Prof. Dr. Hüsnü Özkan
Physics Dept., METU _________________

Prof. Dr. Nizami Hasanli
Physics Dept., METU _________________

Assoc. Prof. Dr. Enver Bulur
Physics Dept., METU _________________

Assist. Prof. Dr. Tacettin Yıldırım
Physics Dept., Nevşehir University _________________

Dr. Demiral Akbar
Physics Dept., METU _________________

Date: May 17, 2010

I hereby declare that all information in this document has been obtained and presented in accordance with academic rules and ethical conduct. I also declare that, as required by these rules and conduct, I have fully cited and referenced all materials and results that are not original to this work.

Name, Last Name : Hisham, Nasser

Signature :

ABSTRACT

THERMALLY STIMULATED CURRENT STUDY OF TRAPS DISTRIBUTION IN TlGaSeS LAYERED SINGLE CRYSTALS

Nasser, Hisham
M. S., Department of Physics
Supervisor: Prof. Dr. Nizami Hasanli

May 2010, 80 pages

Trapping centres and their distributions in as-grown TlGaSeS layered single crystals were studied using thermally stimulated current (TSC) measurements. The investigations were performed in the temperature range of 10–160 K with various heating rates between 0.6–1.2 K/s. Experimental evidence has been found for the presence of three electrons trapping centres with activation energies 12, 20, and 49 meV and one hole trapping centre located at 12 meV. Their capture cross-sections and concentrations were also determined. It is concluded that in these centres retrapping is negligible as confirmed by the good agreement between the experimental results and the theoretical predictions of the model that assumes slow retrapping.

The optical properties of TlGaSeS layered single crystals have been investigated by measuring the transmission and the reflection in the wavelength region between 400 and 1100 nm. The optical indirect transitions with a band gap energy of 2.27 eV and direct transitions with a band gap energy of 2.58 eV were found by analyzing the absorption data at room temperature. The rate of change of the indirect band gap with temperature was determined from the transmission measurements in the temperature range of 10–300 K. The oscillator and the dispersion energies, the oscillator strength, and the zero-frequency refractive index were also reported. The parameters of monoclinic unit cell and the chemical composition of TlGaSes crystals were found by X-ray powder diffraction and energy dispersive spectroscopic analysis, respectively.

Keywords: Thermally Stimulated Currents, Traps, X-ray Diffraction, Energy Dispersive Spectral Analysis, Optical Constants.

ÖZ

TlGaSeS TEK KRİSTALLERDE TUZAK DAĞILIMLARININ ISILUYARILMIŞ AKIM ÇALIŞMASI

Nasser, Hisham
Yüksek Lisans, Fizik Bölümü
Tez Yöneticisi: Prof. Dr. Nizami Hasanli

Mayıs 2010, 80 sayfa

Katkılanmamış TlGaSeS katmanlı tek kristallerindeki tuzak seviyeleri ve dağılımları ısıluyarılmış akım ölçümleri kullanılarak gerçekleştirildi. Araştırmalar 10–160 K sıcaklık aralığında ve 0.6–1.2 K/s aralığındaki çeşitli ısıtma hızları ile yapıldı. Deneysel veriler aktivasyon enerjileri 12, 20 ve 49 meV olan üç elektron ve aktivasyon enerjisi 12 meV olan bir deşik tuzak merkezinin bulunduğunu gösterdi. Bu tuzak seviyelerinin yakalama kesit alanları ve tuzak yoğunlukları bulundu. Deneysel sonuçlar ile yavaş geri tuzaklanmaya ait teorik öngörülerin uyumlu olması bu tuzak seviyelerinde geri tuzaklanmanın ihmal edilebilir olduğunu gösterdi.

TlGaSeS katmanlı tek kristallerinin optiksel özellikleri 400–1100 nm dalgaboyu aralığında gerçekleştirilen geçirgenlik ve yansıtıcılık ölçümleri ile araştırıldı. Oda sıcaklığındaki emilme verilerinin analizleri sonucunda optiksel dolaylı bant geçiş enerjisi 2.27 meV ve doğrudan bant geçiş enerjisi 2.58 meV olarak bulundu. 10–300 K sıcaklık aralığında gerçekleştirilen geçirgenlik ölçümleri sonucunda dolaylı bant aralığının sıcaklık ile değişim oranı bulundu. Ayrıca titreşim ve dağılma enerjileri, titreşim büyüklüğü ve sıfır frekans kırılma indisi belirtildi. TlGaSeS kristalinin monoklinik birim hücre parametreleri ve kimyasal bileşimi X-ışını toz difraksiyon çalışması ve enerji dağılımlı spektrum analizi ile belirlendi.

Anahtar Kelimeler: Isıluyarılmış Akım, Tuzaklar, X-ışını Kırınımı, Enerji Dağılımlı Spektrum Analizi, Optik Sabitler.

ACKNOWLEDGMENTS

First and foremost I offer my sincerest gratitude to my supervisor, Prof. Dr. Nizami Hasanli, who has supported me throughout my thesis with his patience and knowledge whilst allowing me to develop an understanding of the subject. I attribute the level of my Master degree to this encouragement and effort and with him this thesis, too, would not have been completed or written. He has made countless productive and useful suggestions in every part of this work, which has greatly benefited from his careful reading and critical comments.

I also wish to thank Prof. Dr. Hüsnü Özkan who provided a constant encouragement and help throughout this work. His continuous support and the facilities of the Superconductivity Laboratory made it possible to complete this work.

I would like to express my deepest gratitude to Assist. Prof. Dr. Tacettin Yıldırım; we shared every step of Thermally Stimulated Current measurements. One simply could not wish for a better or friendlier doctor.

I am endlessly grateful to my lovely family for their love, patience, and understanding. Their positive attitude towards me was the inner power that compels me to fulfil the requirement of my graduate study.

I owe a debt gratitude to my brother, Dr. Mohamad for his valuable support when I needed.

Finally, I offer my regards and blessings to all of those who supported me in any respect during the completion of this work.

to my lovely family...

TABLE OF CONTENTS

CHAPTERS

LIST OF TABLES

TABLES

LIST OF FIGURES

FIGURES

CHAPTER 1

INTRODUCTION

The TlGaSeS compound belongs to the group of layered semiconductors. This crystal is formed from $TlGaS_2$ and $TlGaSe_2$ crystals by the substitution of half of the selenium atoms by sulphur or vice versa [1,2]. TlGaSeS has two dimensional layers arranged parallel to the (001) plane. The bonding between Tl and Se or S atoms in this crystal is an inter-layer and the one between Ga and Se or S is an intra-layer type. The main structural unit of a layer is the $Ga_4S_{10}(Se_{10})$ polyhedron, representing a combination of four elementary tetrahedra $GaS_4(Se_4)$ linked together by bridging Sulfur or Selenium atoms. Tl atoms are located in tri-gonal prismatic voids resulting from a combination of the $Ga_4S_{10}(Se_{10})$ poly-hedra into a layer. These atoms form nearly planar chains along the $[110]$ and the $[1\bar{1}0]$ directions.

The optical, structural and photoelectrical properties of $TlGaS_2$ and $TlGaSe_2$ layered crystals were analyzed in Refs. [3–18]. The indirect and the direct transitions of $TlGaS_2$ and $TlGaSe_2$ form the fundamental absorption edge with $E_{gi} = 2.35-2.46$ eV, $E_{gd} = 2.38-2.54$ eV, and $E_{gi} = 1.83-2.06$ eV, $E_{gd} = 2.11-2.23$ eV, respectively [3,6]. These crystals enters the fabrications of optoelectronic devices due to their structural properties and potential optoelectronic applications as they have high photosensitivity in the visible range of the spectra and high birefringence in conjunction with a wide transparency range of $0.5-14.0$ μm [9].

The effect of impurity centres on the performance of optoelectronic and electronic devices is a well-known subject. In optoelectronic devices such as lasers and LEDs, impurities may introduce irradiative recombination centres thus lowering the internal quantum efficiency of the device or even render light generation impossible, which depends on the density of defects. In the case of electronic devices, defects may introduce scattering centres thus lowering carrier mobility, hence hindering high–frequency operations. There are several experimental techniques to obtain detailed information about the properties of impurity centres in semiconductors, among these techniques, Thermally Stimulated Current (TSC) measurements are somehow easy to perform and give detailed and enough information about different parameter of trap centres [19–21].

TSC has been used in the last decades to analyze various parameters of defect and impurity centres in different crystal. Obtaining these parameter was very useful in fabricating high-quality devices [21,22]. The study of processes in the TSC technique and methods to evaluate the electron trapping parameters picked up with the work of Randall and Wilkins in 1965 [23]. In this work, their theoretical approach was based on the assumption that carriers, which are thermally excited from the trap levels, have a negligible probability of being retrapped. In 1960, Haering and Adams [24] presented another theoretical work which is an extension of the study of Randall and Wilkins. They studied the theory of thermally stimulated currents in the case of slow and fast re-trapping. In 1964, Nicholas and Woods examined the electron trapping parameters from conductivity glow curves in CdS crystals by using the methods which have been proposed in the previous study [25]. Another theoretical paper was presented by Dussel and Bube in 1967 [26]. This paper was based on the detailed theory of TSC for the case of a single type of trap and a single type of recombination centre [26].

In TSC experiments, traps are filled at initial low temperature by band-to-band excitation for both the electrons and holes using appropriate illumination excitation. The trapped electrons/holes are then released to the conduction or valence band by increasing the temperature. The released carriers give rise to a transient increase in the conductivity of the crystal. This increase in the conductivity is reflected in the TSC curve. TSC curve for a single carrier trap is slightly asymmetric curve with a fairly sharp maximum at a given temperature, which depends on the trap parameters such as its depth, capture cross-section, and concentration as well as on the heating rate. Worth to mention, for the consistency in the TSC experiments, the heating rate in TSC measurements is taken as a constant during all the measurements.

The purpose of the thesis is to obtain detailed information concerning trapping centres in undoped TlGaSeS using the well-established technique of TSC measurements. The Thermally Stimulated Current data is analyzed by different means. The traps parameters such activation energy, capture cross section area, attempt-to-escape frequency, and their concentration for all TSC data of TlGaSeS were obtained. In addition to TSC measurements, the optical properties of the TlGaSeS crystal in the wavelength range of 400−1100 nm are presented. The refractive index, the dispersion energy, and the zero-frequency dielectric constant, and refractive index are identified by means of the room-temperature reflectance and transmittance data. The rate of the change of the indirect band gap with temperature was determined from the temperature dependence of the transmission spectra in the 10–300 K range. Moreover, the results of the energy dispersive spectroscopic analysis and X-ray analysis in the Bragg-angle (2θ) range of $10-75^0$ was used to determine the atomic composition ratio and lattice parameters of the TlGaSeS crystals, respectively.

CHAPTER 2

THEORETICAL APPROACH

2.1 Introduction

Material can be classified according to their electrical properties into conductors and insulators. Semiconductors are thermally stimulated insulator; under the effect of light, heat, and voltage. At 0 K a huge amount of free charge carriers, even million times smaller than the number of free charge carriers in conductors, exits. Devices made from semiconductor materials are the foundation of modern electronics, including radio, computers, telephones, and many other devices. Semiconductor devices include the various types of transistor, solar cells, many kinds of diodes including the light-emitting diode, the silicon controlled rectifier, and digital and analog integrated circuits. Consequently, it is of great importance to get enough information about the characteristics and behaviours of semiconductors under different conditions because of their importance in technology.

The main purpose of this chapter is to give a literature review about some basic properties of semiconductors, thermally stimulated current technique used to analyze the trapping centres of semiconductors, and some other characterization techniques used for the analysis of semiconductors.

2.2 Electrical Properties of Semiconductors

2.2.1 Band Structure

The conductivity of different materials depends on their band structure. The electrons in semiconductors and insulators can have energies only within certain bands(i.e. ranges of levels of energy) between the energy of the ground state, corresponding to electrons tightly bound to the atomic nuclei of the material, and the free electron energy, which is the energy required for an electron to escape entirely from the material. The energy bands each correspond to a large number of discrete quantum states of the electrons, and most of the states with low energy (closer to the nucleus) are full, up to a particular band called the valence band. The valence band in the semiconductor materials is nearly filled under usual operating conditions, thus causing more electrons to be available in the "conduction band" under external excitations; the conduction band is the band immediately above the valence band. Electrons in the conduction band can move freely throughout the solid. Thus, the conductivity of a material is proportional to the number of electrons in the conduction band. Band gap is defined as the energy difference between the valence and conduction bands. The band gap of a semiconductor material is less than that of insulator but higher than that of conductors. Figure 2.1 shows a simple model comparing the band gap of each type of material. The valence band electrons in semiconductors can be excited to the conduction band when they gain enough energy from external source. The electrons excited to the conduction band increase the conductivity of the semiconductor material. This controllable conductivity property of the semiconductors has tremendously important role in many technological areas. Typically, band gap of semiconductors is less than 3 eV and insulators have higher band gap energy that is usually greater than 3 eV.

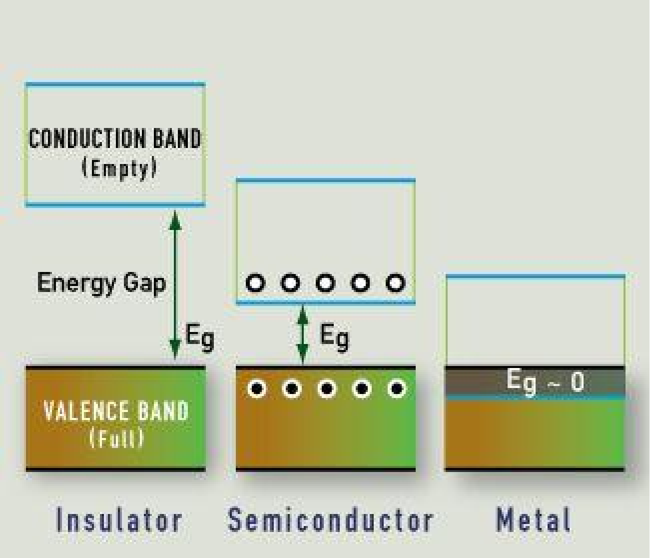

Fig. 2.1. The relative comparison of band gap energies of conductors, insulators and semiconductors.

2.2.2 Defects

Crystals in the nature are never perfect. All crystals have some defects or irregularities in their ideal arrangements. Although it seems that defects cause problems, they have an important role in the use of materials in the semiconductor science and determine many properties of the materials.

There are mainly two types of crystal defects called as point defects and line defects-dislocations [27].

Point defects are the dimensionless defects where an atom is missing at one or more lattice locations or is in an irregular place in the lattice structure. There exist mainly four kinds of point defects in the crystal lattice. All these kinds of defects are shown in the figure 2.2.

i. Self interstitial atoms: These are extra atoms which are the same type with the atom already present in the lattice and sit in an interstitial position.

ii. Interstitial impurity atoms: These are the atoms, which are smaller than the atoms in the crystal and fit into the open space between the bulk atoms of the lattice structure.

iii. Substitutional impurity atoms: These are the different type of atoms in the lattice structure instead of the bulk atom.

iv. Vacancies: Vacancies exist when an atom is missing at one or more lattice sites. These missing atoms leave an empty region in its place.

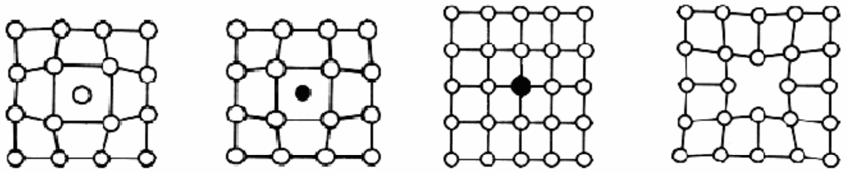

Fig. 2.2. (i) Self interstitial atom, (ii) Interstitial impurity atom, (iii) Substitutional impurity atom, (iv) Vacancy [27].

In the line defects, groups of atoms are in irregular positions. Line defects are also called dislocations. There are two types of dislocations:

(a) Edge dislocation: This dislocation exists when an extra half-plane of atoms is replaced in or removed from the crystal structure (figure 2.3a).

(b) Screw dislocation: If the dislocation is formed by the displacement of atoms in a plane in the crystal then a screw dislocation is observed. A step or ramp is formed in this type of dislocation (figure 2.3b).

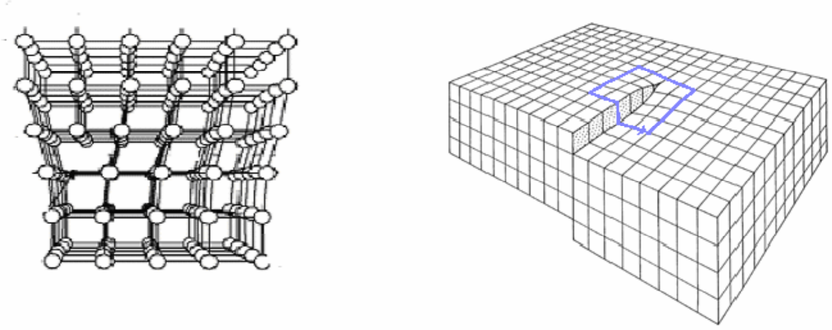

Fig. 2.3. (a) Cross section of an edge dislocation, which extends into the page; (b) Screw dislocation [26].

2.3 X-ray Diffraction Experiments

X-rays are electromagnetic waves with a wavelength in the range of 10^{-8} to 10^{-11} m and this wavelength is of the same order of magnitude with the spacing between the planes of crystal. Thus X-rays are used to produce diffraction pattern. X-ray diffraction experiments are utilized to obtain information about the interplanar spacing between planes of atoms, the crystal structure of an unknown material and the orientation of a crystal.

The theoretical explanation of X-ray diffraction experiment is as follows: X-rays are radiated onto a material, which consists in crystals with a spacing d between its planes (figure 2.4). These X-rays will be reflected after colliding with the electrons in the crystal lattice. According to the law of reflection, the angle of incident light θ will be equal to the angle of reflection. The reflection of X-rays from different atoms causes a path difference between them. The path difference between any two successive rays is equal to

$$|AB| + |AC| = 2d \sin\theta . \tag{2.1}$$

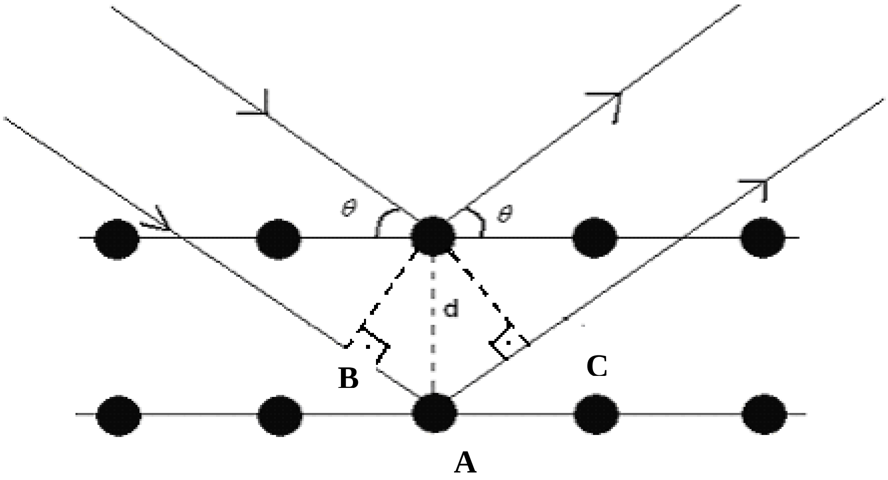

Fig. 2.4. Representation of X-ray diffraction by a crystal lattice.

X-rays scattered from different atoms constitute constructive or destructive interference due to their path differences. If the path difference between any two rays is an integer multiple of the wavelength (λ) of emitted X-rays, these rays interfere constructively. The mathematical relation of this constructive interference is called "Bragg's law" and given by the expression [28]

$$2d_{hkl} \sin\theta = n\lambda \ , \qquad n = 0,1,2,3.... \tag{2.2}$$

where n is an integer.

The interplanar spacing d depends only on the type and size of the unit cell and Miller indices. Bragg's law and expression to find the d from the Miller indices can be combined for different kind of crystals to determine the lattice parameters. The interplanar spacing *d* as a general form is given by the expression

$$\frac{1}{d_{hkl}^2} = \frac{1}{\left[1 + 2\cos(\alpha)\cos(\beta)\cos(\gamma) - \cos^2(\alpha) - \cos^2(\beta) - \cos^2(\gamma)\right]}$$
$$\times \left[\frac{h^2 \sin^2(\alpha)}{a^2} + \frac{k^2 \sin^2(\beta)}{b^2} + \frac{l^2 \sin^2(\gamma)}{c^2} \right.$$
$$+ \frac{2hk}{ab}(\cos(\alpha)\cos(\beta) - \cos(\gamma)) + \frac{2kl}{bc}(\cos(\beta)\cos(\gamma) - \cos(\alpha))$$
$$\left. + \frac{2lh}{ac}(\cos(\gamma)\cos(\alpha) - \cos(\beta)) \right] , \qquad (2.3)$$

where *a*, *b* and *c* are lattice constants, *h*, *k* and *l* are Miller indices and *α*, *β*, and *γ* are the angles for the lattice structure.

2.4 Energy Dispersive Spectral Analysis Experiments

Energy dispersive spectral analysis (EDSA) also called energy dispersive X-ray analysis (EDXA) is an analytical method used to get information about the chemical characterization of any sample. As a spectroscopy technique, EDSA mainly depends on the interaction between electromagnetic radiation and sample. The basic physical principle of EDSA technique is described as follows:

When a sample is bombarded with a particle beam such as electron beam, the ground state electrons within the atom are excited to an inner shell. The excited electron leaves a hole within the atom’s electronic structure. Then an outer shell electron fills this hole by exposing energy. The excess energy of this transmission is emitted as X-ray from the atom. The fundamental principle in EDSA is that every element has a unique atomic structure and this uniqueness allows the emitted X-rays being the characteristic of an element’s atomic structure. Thus, the X-rays emitted by the sample are analyzed to understand the chemical properties of the sample. In addition to knowing the composite elements in a material, EDSA analysis is also used to determine the ratio of each element in the material.

2.5 Optical Absorption, Transmission and Reflection of Semiconductors

Absorption, transmission and reflection experiments are simple methods for evaluating some optical properties of semiconductors. The analysis of such measurements mainly based on the relation between the intensity of incident, transmitted and reflected light which are analyzed within the general behaviour of electromagnetic waves on the surface of different material. This behaviour is governed by Maxwell’s equations.

Absorption: When a light is radiated on a semiconductor, some of the incident light is absorbed through the material if the energy of the light is equal or higher than the band gap energy of the solid. In the absorption process, an electron in the lower energy state is excited to a higher energy state by absorbing the energy of the incident light. The intensity of the incident light decreases after the absorption process. Then the fraction of intensity of the incident light after propagation a distance x through the material is given by [29]

$$\frac{I(x)}{I_0} = \exp(-\alpha x), \tag{2.4}$$

where I_0 is the intensity of the incident light, $I(x)$ is the intensity after this propagation and α is the absorption coefficient defined as

$$\alpha = \frac{4\pi k}{\lambda}, \tag{2.5}$$

where λ is the wavelength of the light wave and k is the absorption index of the material.

The absorption coefficient, α, for a given photon energy hv depends on the probability of the transition from the initial state to final state. The absorption coefficient α, photon energy hv and band gap energy E_g are related by the expression [30]

$$(\alpha hv) = A\left(hv - E_\mathrm{g}\right)^\mathrm{p}, \tag{2.6}$$

where A is a constant depending on the transition probability whereas p is the index characterizing the optical absorption process. The value of the p is equal to 2 for indirect allowed transitions and to 1/2 for the direct one.

Reflection: When light is sent to the material, some of them is reemitted by the material to the incoming plane. This process is called reflection and for normal incidence, the reflection coefficient is given by [29]

$$R = \frac{(n-1)^2+k^2}{(n+1)^2+k^2}, \tag{2.7}$$

where n is the refractive index of the material. In the transparent range in which absorption index k is equal to zero, the reflection coefficient becomes

$$R = \frac{(n-1)^2}{(n+1)^2}, \tag{2.8}$$

Transmission: When the light normally falls on the material, some of them propagate through the material and then leaves the material without changing its direction. This process is called as transmission. The transmission coefficient is defined as the ratio of the intensities of transmitted and incident light and given by [29]

$$T = \frac{(1-R)^2\exp(-\alpha x)}{1-R^2\exp(-2\alpha x)}, \tag{2.9}$$

where x is the thickness of the material. When the product αx is large, then $\exp(-2\alpha x) \approx 0$ and the transmission coefficient is

$$T \cong (1-R)^2\exp(-\alpha x). \tag{2.10}$$

If R and x are known, α can be evaluated from the equation 2.9. If the refractive index n is known, the thickness of the thin sample can be obtained from the transmission interference fringes at wavelengths slightly longer than the absorption edge. The expression describing thickness from this method is [29]

$$\mathrm{x} = \frac{1}{2\mathrm{n}}\left(\frac{\lambda_1\lambda_2}{\lambda_1-\lambda_2}\right), \tag{2.11}$$

where λ_1 and λ_2 are the position of the two neighbouring peaks.

Moreover, the dispersive refractive index data for $h\nu < E_\mathrm{g}$ can be determined according to the single-effective-oscillator model proposed by Wemple and DiDomenico [31,32]. In this model, the refractive index is related to photon energy through the relation

$$n^2 = 1 + \frac{E_\mathrm{so}E_\mathrm{d}}{\mathrm{E}_\mathrm{so}^2-(h\nu)^2}, \tag{2.12}$$

where E_so is the single oscillator energy and E_d is the dispersion energy. E_so and E_d parameters are evaluated from the graph of $(n^2-1)^{-1}$ versus $(h\nu)^2$ by fitting a linear function to the lower energy range. Also the zero-frequency refractive index n_0 is obtained from the equation 2.12 by replacing $h\upsilon = 0$. The expression for n_0 is obtained as

$$n_0^2 = 1 + \frac{E_\mathrm{d}}{E_\mathrm{so}}, \tag{2.13}$$

2.6 Thermally Stimulated Current

2.7.1 Introduction

Thermally stimulated processes cover a number of some physical techniques in which the sample is heated and a property of the sample is measured as a function of temperature. The result of such a measurement is a curve of measured parameter versus time or temperature. The analysis of this curve is used in many areas of physics and chemistry to determine various properties of materials. The most important thermally stimulated processes are the following [33–38]:

i. Thermoluminescence
ii. Thermally stimulated current (TSC)
iii. Thermally stimulated electron emission
iv. Deep level transient spectroscopy
v. Thermally stimulated depolarization current

The thermally stimulated current is the current generated from a semiconductor when it is heated following the previous absorption of energy from radiation. There are three essential ingredients necessary for the production of TSC:

a. The material must have trapping levels in its band gap
b. The material must have at some time absorbed energy during exposure to radiation
c. The TSC generation is triggered by heating the material

The thermally stimulated current is extensively used to get information on the impurity and defect centres in the crystal. In this method, the sample excited previously at an initial low temperature is heated under the voltage applied across the contacts connected to the sample. While heating the sample linearly, the transient electric currents in the sample are measured as a function of the temperature. The resulting curve is called a TSC curve and usually in the form of peak(s), giving information about the properties of shallow and/or deep trapping levels within the band gap.

2.7.2 Transitions in the Thermally Stimulated Current Process

The possible transitions of electrons in the band gap are the main physical events considered in the TSC experiments. The major electronic transitions associated with the TSC are described below and represented in the figure 2.5.

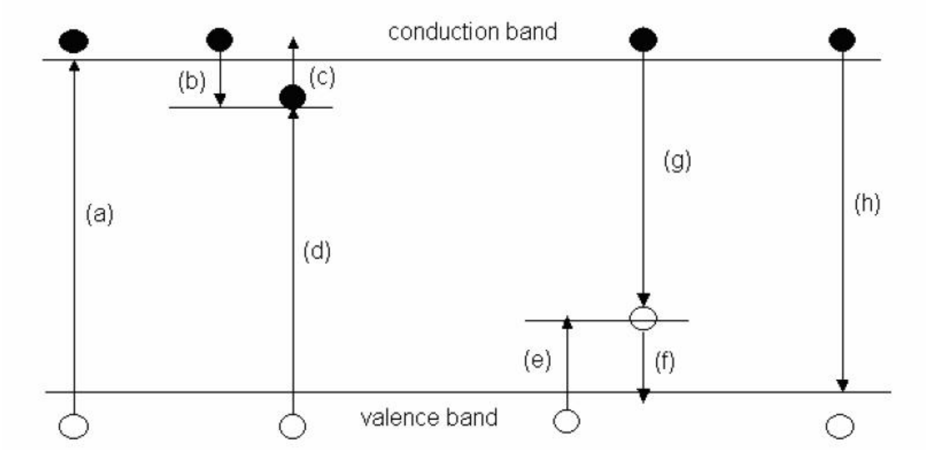

Fig. 2.5. Possible electronic transitions in the TSC technique. (a) band-to-band excitation; (b) and (e) electron and hole trapping, respectively; (c) and (f) electron and hole release, respectively; (d) and (g) indirect recombination; (h) direct recombination. Solid circles, open circles and arrows represent electrons, holes and transitions, respectively [33].

i. Transition (a) is the band-to-band excitation of a valence band electron to conduction band. This transition occurs when valence band electron is given enough energy from an external source.

ii. Transitions (b) and (e) are called as electron and hole trapping, respectively. Excited electrons and holes in the conduction and valence bands will return to their initial band. Through this return some of the electrons and holes are trapped at trapping centers.

iii. Transitions (c) and (f) are called as electron and hole releases. When enough energy is given to electrons and holes in the trapping centers, they are excited to conduction or valence bands, respectively.

iv. Transitions (g) and (d) are indirect recombination mechanisms. These transitions occur when free electrons and holes in the conduction and valence bands, respectively, recombine with a charge carrier of opposite sign in the trapping centers.

v. Transition (h) is the direct recombination defined as the recombining of a charge carrier in the conduction band with the opposite sign charge carrier in the valence band.

The following simple model can explain the TSC method: The electrons are excited by some kind of radiation from the valence band to the conduction band at an initial low temperature (transition a). Most of the electrons in the conduction band return to the ground state in a short time (transition h). Some of them are trapped in the trapping centres associated with the lattice defects such as vacancies, interstitials or impurities (transition b). A hole is created in the valence band in the place of electron trapped in the trapping center. These holes are also trapped in the hole trap centres (transition e). These trap electrons (holes) return back to conduction (valence) band when a sufficient energy is given (transitions c and f). In the thermally stimulated processes the type of the given energy is thermal energy. The electrons excited to the conduction band give a transient increase in the conductivity of the sample. This increase is observed as a peak in the TSC curve of the sample. The analyses of the peak(s) give information about the some properties of the trap levels such as activation energy and concentration of electrons in these centres.

2.7.3 Theoretical Approach

At a temperature T, the probability P that an electron can be released back into the conduction band from a trap depth of E (transition c) is given by

$$P = \nu \exp(-E/\kappa T), \tag{2.14}$$

where ν is the attempt-to-escape frequency and κ is the Boltzmann constant. In a semiconductor, the former is defined by the expression

$$\nu = N_{\mathrm{c}} \upsilon S_{\mathrm{t}}\ , \tag{2.15}$$

where S_{t} is the capture cross section, N_{c} and υ are the effective density of states in the conduction band and thermal velocity of the conduction electrons, respectively. N_{c} and υ are given by

$$N_{\mathrm{c}}(T) = 2\left(\frac{\kappa T m_{\mathrm{e}}^{*}}{2\pi n}\right)^{2/3}, \tag{2.16}$$

and

$$v(T) = \sqrt{\frac{3\kappa T}{m_{\mathrm{e}}^{*}}}, \tag{2.17}$$

where m_{e}^{*} is the electron effective mass [29].

The concentration of filled traps (n) mainly depends on the transitions from or to trapping center. These possible transitions and their theoretical explanations are [33]:

i. **Stimulation** (transition c): The transition from the trapping center to the conduction band affects the concentration of filled traps. Decrease of trapped electron population is dependent on the concentration n and given by the relation

$$\frac{\mathrm{d}n}{\mathrm{d}t} \propto -n\nu\exp(-E/\kappa T), \tag{2.18}$$

ii. **Re-trapping**: In addition to the excitation transition we should also take into account the re-trapping (transition b). The probability of re-trapping process depends on both the concentration of free electrons n_c in the conduction band and the concentration of unoccupied traps $(N - n)$, where N is the total concentration of traps. The relation describing the effect of re-trapping on the rate of change of trapped electron concentration is

$$\frac{\mathrm{d}n}{\mathrm{d}t} \propto n_{\mathrm{c}}(N - n)S_{\mathrm{t}}v, \tag{2.19}$$

The total rate of change of electron concentration can be obtained as

$$\frac{\mathrm{d}n}{\mathrm{d}t} = n_{\mathrm{c}}(N - n)S_{\mathrm{t}}v - n\nu\exp(-E/\kappa T). \tag{2.20}$$

by combining equations 2.18 and 2.19.

An electron excited to the conduction band can either be trapped or recombine with a hole, directly or through a recombination center. The rate of the recombination is n_c/τ, where τ is defined as recombination lifetime. Then the rate of change of the free electrons concentration n_{c} is equal to

$$\frac{\mathrm{d}n_{\mathrm{c}}}{\mathrm{d}t} = -\frac{n_{\mathrm{c}}}{\tau} - \frac{\mathrm{d}n}{\mathrm{d}t}\,. \tag{2.21}$$

For the solution of equations 2.20 and 2.21, two fundamental assumptions have been suggested:

1. Slow Re-trapping: As suggested by Randall and Wilkins [23], in this case the re-trapping of a charge carrier is negligible compared to the rate of recombination and the electron released to the conduction band recombines quickly with a hole. This assumption also called as “first order kinetics” is expressed by the following inequalities:

$$\frac{n_{\mathrm{c}}}{\tau} \gg n_{\mathrm{c}}(N-n)S_{\mathrm{t}}v \tag{2.22}$$

and

$$\left|\frac{\mathrm{d}n_{\mathrm{c}}}{\mathrm{d}t}\right| \ll \left|\frac{\mathrm{d}n}{\mathrm{d}t}\right|. \tag{2.23}$$

Using equations 2.22 and 2.23, equation 2.20 becomes

$$\frac{\mathrm{d}n}{\mathrm{d}t} \approx -n\nu\exp(-E/\kappa T), \tag{2.24}$$

and

$$\frac{\mathrm{d}n}{\mathrm{d}t} \approx -\frac{\mathrm{n}_c}{\tau}. \tag{2.25}$$

Integrating equation 2.24 by assuming a linear heating function $T = T_\mathrm{o} + \beta t$, we get

$$n = n_0 \exp\left\{-\int_{\mathrm{T}_0}^{\mathrm{T}} \frac{\nu}{\beta} \exp(-E/\kappa T)\mathrm{d}T\right\}, \tag{2.26}$$

where n_0 is the initial trapped electron concentration at initial temperature T_0.

Then substituting equations 2.25 and 2.26 into equations 2.24, we get

$$n_\mathrm{c} = n_0 \tau \nu \exp\left\{-\frac{E}{\kappa T} - \int_{\mathrm{T}_0}^{\mathrm{T}} \frac{\nu}{\beta} \exp(-E/\kappa T)\mathrm{d}T\right\}, \tag{2.27}$$

the thermally stimulated conductivity σ is given by

$$\sigma = n_\mathrm{c} e \mu = n_0 \tau \nu e \mu \exp\left\{-\frac{E}{\kappa T} - \int_{\mathrm{T}_0}^{\mathrm{T}} \frac{\nu}{\beta} \exp(-E/\kappa T)\mathrm{d}T\right\}, \tag{2.28}$$

where τ is a free charge carrier lifetime, μ is its mobility, β is the heating rate, and T_0 is the initial temperature. Then the thermally stimulated current is described by the equation

$$I = n_0 \tau \nu e \mu \left(\frac{V}{L}\right) A \tau \nu e \mu \exp\left\{-\frac{E}{\kappa T} - \int_{\mathrm{T}_0}^{\mathrm{T}} \frac{\nu}{\beta} \exp(-E/\kappa T)\mathrm{d}T\right\}, \tag{2.28a}$$

where V is the bias voltage, A is the area of the sample and L is its length.

2. Fast Re-trapping: Haering and Adams (1960) considered the case in which the time required for thermal equilibrium between the conduction electrons and trapped electrons is much shorter than the recombination lifetime [24]. If we show the total number of electrons by

$$n_{\mathrm{t}} = n + n_{\mathrm{c}}, \tag{2.29}$$

and assume

$$N \gg N_{\mathrm{c}}\exp(-E/\kappa T), \tag{2.30}$$

for fast trapping process, then the rate of change of total electrons is

$$\frac{\mathrm{d}n_{\mathrm{t}}}{\mathrm{d}t} = -\frac{n_{\mathrm{c}}}{\tau} = -\frac{n_{\mathrm{t}}}{\tau}\left(\frac{N_{\mathrm{c}}}{N}\right)\exp\left(-\frac{E}{\kappa T}\right), \tag{2.31}$$

Where n and n_{c} are concentration of electrons in traps and conduction band, N and N_{c} are concentration and effective concentration of trapping and conduction states, respectively, and τ is the recombination lifetime. The solution of the equation 2.31 is [33]

$$n = n_0\exp\left[-\frac{1}{\beta}\int_{\mathrm{T}_0}^{\mathrm{T}}\frac{N_{\mathrm{c}}}{N\tau}\exp(-E/\kappa T)\mathrm{d}T\right], \tag{2.32}$$

and the thermally stimulated current is

$$I = \left(\frac{V}{L}\right)A\frac{N_{\mathrm{c}}\mu}{N}en_0\exp\left\{-\frac{E}{\kappa T} - \frac{N_{\mathrm{c}}}{N\beta\tau}\int_{\mathrm{T}_0}^{\mathrm{T}}\exp(-E/\kappa T)\mathrm{d}T\right\}. \tag{2.33}$$

2.7.4 Curve Fitting

(i) Slow Re-trapping: The TSC peak of traps for the first order kinetics is described by the equation 2.28a. If it is assumed that ν is independent of temperature T and the variation of μ and τ is negligible with temperature range of TSC experiment, equation 2.28a can be rewritten as [39]

$$I = \left(\left(\frac{V_2}{L}\right)A\right)A_0\exp\left\{-t + B'\int_{t_0}^{t}\exp(-t)t^{-2}dt\right\}, \tag{2.34}$$

where , V_2 is the applied voltage $t = \frac{E}{\kappa T}$ and, A_0 and B' are constant:

$$A_0 = n_0\tau e\mu\nu \quad \text{and} \quad B' = \frac{\nu E_t}{\beta\kappa}, \tag{2.35}$$

where n_0 is the initial density of traps. If we integrate relation 2.34 by parts several times, we get a convergent infinite series expression;

$$I = \left(\left(\frac{V_2}{L}\right)A\right)A_0\exp\left[-t - B'\{\exp(-t)t^{-2} - 2\exp(-t)t^{-3} + 3\times 2\exp(-t)t^{-4}\ldots\}_{t_0}^{t}\right]. \tag{2.36}$$

Because t is large in practice, by making approximation, the infinite series can be written as

$$I \approx \left(\left(\frac{V_2}{L}\right)A\right)A_0\exp[-t - B'\exp(-t)t^{-2}] \tag{2.37}$$

$$I \approx I_0 + \left(\left(\frac{V_2}{\mathrm{L}}\right) A\right) A_0 \exp[-t - B' \exp(-t) t^{-2}] \,, \tag{2.38}$$

where I_0 is the value at t_0 . If we differentiate relation 2.38 and set it to zero to obtain the maximum of the curve, which occurs at

$$t = t_{\mathrm{m}} = \frac{E_{\mathrm{t}}}{\kappa T_{\mathrm{m}}} \tag{2.39}$$

then

$$B' = \exp(t_{\mathrm{m}}) \frac{t_{\mathrm{m}}^3}{t_{\mathrm{m}}+2} \,. \tag{2.40}$$

(ii) Fast Re-trapping: In the equation 2.33 for second order kinetics given by Haering and Adams, if we insert $t = \frac{E}{\kappa T}$ it becomes [40]

$$I = \left(\frac{V_2}{L}\right) AC \left[-t + D \int_{\mathrm{t}_0}^{\mathrm{t}} \exp(-t) t^{-7/2} \, dt\right], \tag{2.41}$$

where

$$C = \frac{N_{\mathrm{C}} e \mu n_0}{N} \quad \text{and} \quad D = \frac{N_{\mathrm{C}} E^{5/2}}{N \beta T^{*3/2} \kappa^{5/2} \tau} \,. \tag{2.42}$$

Integrating relation 2.41 by parts, and then approximating gives

$$I \approx C \exp\left[-t - D \exp(-t) t^{-7/2}\right] \tag{2.43}$$

If we differentiate equation 2.43 and then set it to zero we obtain the value of t^* at the maximum, D^* is found as

$$D^* = \frac{\exp(t^*)t^{*9/2}}{t^*+3.5} \tag{2.44}$$

where D^* is the value of D to the limits of the approximation used.

Simultaneous peaks can be analyzed by the following fitting function

$$I(T) = \sum_{\mathrm{i}=1}^{\mathrm{n}} I_{\mathrm{i}}(T) \tag{2.45}$$

where $I_{\mathrm{i}}(T)$ is the TSC of each peak calculated by using either the relation 2.38 or 2.43 for slow and fast re-trapping, respectively, and n represents the number of trapping centres contributing in the calculation.

When TSC curve are fitted and both E_{t} and T_{m} for peaks are obtained, relation 2.40 or 2.44 can be used to calculate B' or D^* for slow and fast re-trapping processes, respectively. Also for the first order kinetics, the attempt-to-escape frequency ν can be obtained by mean of relation 2.35. Then the cross section of the traps can be calculated using the value of ν and the following expression

$$S_{\mathrm{t}} = \frac{\nu}{N_{\mathrm{c(v)}}\upsilon_{\mathrm{th}}} \tag{2.46}$$

here, $N_{\mathrm{c(v)}}$ is the effective density of states in the related band and υ_{th} is a free charge carrier thermal velocity.

The concentration of the traps can be estimated using the relation [41]

$$N_{\mathrm{t}} = \frac{Q}{ALeG} \tag{2.47}$$

where, Q is the quantity of released charge in a Thermally Stimulated Current measurement. Q can be obtained from the area under the obtained peaks; e is the electronic charge, and G is the photoconductivity gain, which equals to the number of electrons flowing within the crystal for each absorbed photon.

To calculate G the following relation can be used [22]

$$G = \frac{\tau}{t_{\mathrm{tr}}} = \frac{\tau \mu V_2}{L^2} \tag{2.48}$$

here, τ is the electron or hole lifetime, t_{tr} is their transit time between the electrodes, and μ is their mobility. When we irradiate the sample by initial illumination light, electron-hole pairs are generated and material conductivity is changed due to this electron-hole pair generation. The electrons and holes will flow towards the opposite directions by the electric field present in the crystal, thus a current is produced. The free charge carriers appear in the crystal until they either recombine with an opposite charge carrier or are collected at the contacts. G in the crystals arises because the each charge carrier travels within circuit many times until it recombines with an oppositely charged carrier. Each time the charge carrier goes through the circuit it contributes to the current. The photoconductivity gain is given by relation 2.48

2.7.5 Initial Rise Method

Garlick and Gibson [25] first presented this method in 1948. Because initial rise method is independent of the recombination kinetics, it is an attractive method in the analysis of the TSC curves. The integrals in the first and second order equations 2.28a and 2.33 are very small when the traps begin to empty as the temperature is increased. Therefore, exponential terms in these integrals are very close to unity in this temperature range of the process. So the current is written as

$$I = C\exp(-E/\kappa T) \tag{2.49}$$

where C is constant. When the initial portion of the TSC curve is analyzed, the plot of $\ln(I)$ as a function of $1/T$ gives a straight line which has a slope of $(-E_{\mathrm{t}}/\kappa)$. The limitation of this method is that there must be no overlap peak in the initial rise portion of the analyzed peak.

2.7.6 Peak Shape Method (Chen Method)

In the peak shape method, the activation energy of trap is associated by using three parameters (figure 2.6): $\tau = T_{\mathrm{m}} - T_{\mathrm{l}}$, $\delta = T_{\mathrm{h}} - T_{\mathrm{m}}$, $w = T_{\mathrm{h}} - T_{\mathrm{l}}$, where T_{m} is the temperature corresponding to the maximum current, T_{l} and T_{h} are the low and high half-intensity temperatures, respectively [33].

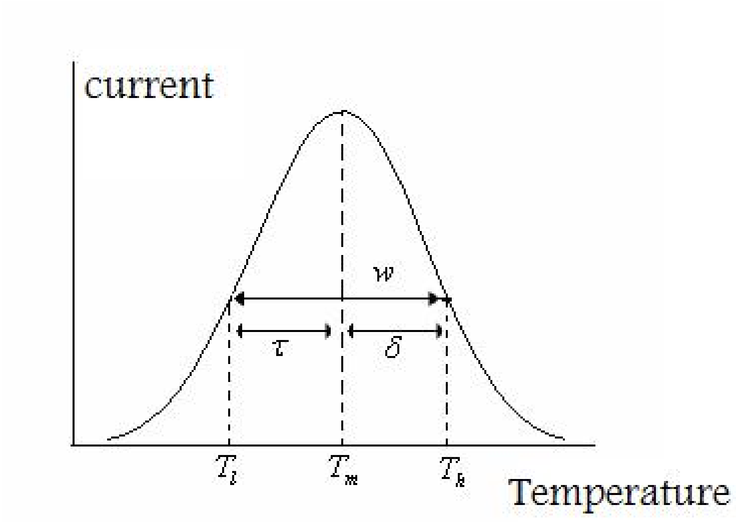

Fig. 2.6. Representation of parameters used in peak shape method.

The activation energy of the trap is obtained by

$$E_\tau = \left[1.51 + 3.0\left(\mu_\mathrm{g} - 0.42\right)\right] \kappa T_\mathrm{m}^2/\tau - \left[1.58 + 4.2\left(\mu_\mathrm{g} - 0.42\right)\right] 2\kappa T_\mathrm{m} \tag{2.50}$$

$$E_\delta = \left[0.976 + 7.3\left(\mu_\mathrm{g} - 0.42\right)\right] \kappa T_\mathrm{m}^2/\delta \tag{2.51}$$

$$E_\mathrm{w} = \left[2.52 + 10.2\left(\mu_\mathrm{g} - 0.42\right)\right] \kappa T_\mathrm{m}^2/w - 2\kappa T_\mathrm{m}, \tag{2.52}$$

where μ_g is equal to ratio δ/w. In 1960 Halperin and Braner suggested to use μ_g value to understand the order of kinetics. The values of μ_g were predicted by Chen and Kirsh [33] as 0.42 and 0.52 for first and second-order kinetics, respectively. The peak shape method cannot be carried out on the curve, which contains more than one peak. If such a curve occurs, the analyzed peak can be cleaned from the other satellite peaks.

2.7.7 Isothermal Decay Method

This method is based on the shape of the decay curve with time. The procedure of the method is as follows: The sample is heated and then it is held at a constant temperature T_{p}. The thermally stimulated current can be described for this process by [33]

$$I = I_0 \exp(-\gamma t) \tag{2.53}$$

where I_0 is the initial current at time $\mathrm{t} = 0$ and

$$\gamma = \nu \exp\left(-E_{\mathrm{t}}/\kappa T_{\mathrm{p}}\right) \tag{2.54}$$

Then the measurement is repeated at different values of temperature T_{p} and for all measurements, γ values are evaluated from the slopes of the plots $\ln(I)$ versus time t graph. The ln values of the slopes can now be plotted as a function of $1/T$ and a straight line with a slope of $(-E_{\mathrm{t}}/\kappa)$ is obtained.

2.7.8 Traps Distribution

Most analysis of the thermally stimulated current mentioned above is based on the assumption that the trapping centres which are related to a specific defect have the same, discrete activation energy. However this assumption is not acceptable for all crystals. Especially in amorphous semiconductors it is observed that the band gap of these semiconductors contains a finite density of available states. Mott and Davies [42] explained this picture by the assumption of the presence of localized states.

For the study of the traps distribution, we assume an exponential distribution of traps whose density at energy E is expressed by [43]

$$N(E) = A\exp(-\alpha_1 E), \tag{2.55}$$

where α_1 is the energy parameter characterizes the distribution. Then, for this exponential distribution, we can write for the traps filled at the excitation temperature T_e

$$n_0(T_\mathrm{e}) = A\exp(-\alpha_1 E)\exp[(E - E_\mathrm{f})/\kappa T_\mathrm{e}], \tag{2.56}$$

where E is the Fermi level energy in darkness and E_f is the energy of the quasi-Fermi level for electrons during light excitation. E and E_f are written as

$$E = \kappa T_\mathrm{m}\ln[N_\mathrm{c}/n_\mathrm{m}]. \tag{2.57}$$

and

$$E_\mathrm{f} = \kappa T_\mathrm{m}\ln[N_\mathrm{c}/n_\mathrm{e}], \tag{2.58}$$

where n_m and n_e are the densities of free electrons at temperature T_m in darkness and during light excitation, respectively. n_0 is proportional to the area of the TSC curve, by assuming this exponential trap distribution, whose density is given by equation 2.55, we can write equation 2.57 for traps filled at the excitation temperature T_0 as

$$S_0(I_\mathrm{m}/I_\mathrm{e}) \propto A\exp(-\alpha_1 E), \tag{2.59}$$

where α_1 is the energy parameter which characterizes the distribution, S_0 is the area of the Thermally Stimulated Current peak, I_m is the current flowing in the sample at the peak temperature in darkness and I_e current flowing in the sample at the peak temperature during light excitation.

CHAPTER 3

EXPERIMENTAL DETAILS

3.1 Introduction

X-ray diffraction and Energy dispersive spectral analysis, transmission, reflection, thermally stimulated current and photoconductivity decay measurements were carried out on as-grown TlGaSeS layered single crystals. TlGaSeS polycrystals were synthesized from high pure elements (at least 99.9999%) prepared in stoichiometric proportions. TlGaSeS layered crystals were grown using the Bridgman method. Good optical quality and freshly cleaved surfaces, which were mirror-like, were revealed by the resulting ingot. No intentional doping of the crystal was performed.

3.2 Energy Dispersive Spectral Analysis and X-ray Diffraction Experiments

The chemical composition of TlGaSeS crystal was determined by means of an energy dispersive spectroscopic analysis (EDSA) by using a JSM-6400 scanning electron microscope. The equipments of the device, “NORAN System6 X-ray Microanalysis System” and “Semafore Digitizer”, were used for the analysis of the experimental data.

X-ray diffraction technique was used to obtain information about the structural parameters of TlGaSeS. A “Rigaku Miniflex” diffractometer with CuKα radiation having λ = 0.154049 nm was used at a scanning speed of 0.02°/sec for the X-ray powder diffraction experiments. The crystal system, the lattice parameters, and Miller indices of the diffraction peaks, were evaluated by using a least-squares computer program “DICVOL 04”.

3.3 Transmission and Reflection Measurements

Transmission and reflection measurements were performed in the 400–1100 nm wavelength region by using a “Shimadzu” UV 1201 model spectrophotometer, which consisted of a 20 W halogen lamp, a holographic grating and a silicon photodiode. It has 5 nm resolutions. Transmission measurements were done under normal incidence of light with a polarization direction along the (001) plane, which is perpendicular to the *c*-axis of the crystal. We utilized the specular reflectance measurement attachment with a 5° incident angle for the room temperature reflection experiments. The sample was cooled from room temperature down to 10 K, within an accuracy of ∓0.5 K, by using an “Advanced Research Systems, Model CSW-202” closed cycle helium cryostat.

3.4 Thermally Stimulated Current (TSC) Experiments

3.4.1 Introduction

In a TSC experiment, TlGaSeS layered single crystal was cooled down to low temperature and was irradiated using a light source which excites carriers across the band-gap. Traps are filled by band-to-band excitation of the excited carriers (transitions b and e in figure 2.5 for electron and hole traps respectively). The trapped charge carriers remain in the trap centres until a sufficient amount of thermal energy is applied through heating to excite these charged carriers to their respective delocalized conduction (valence) band (transitions c and f in figure 2.5 for electron and hole traps respectively). Heating the sample is normally done on a linear time scale at a heating rate β (i.e. $T = T_0 + \beta$t). This heating rate is usually desired to be constant for the same of convenience in the analysis of the TSC peak(s). When a sufficient amount of thermal energy is given, the charge carriers electron (holes) are thermally excited to the conduction (valence) bands, they give rise to a transient increase in the conductivity of the crystal.

3.4.2 Sample Preparation

TlGaSeS crystals of dimensions of 9.0 mm × 10 mm × 0.8 mm were used for TSC measurements. We made the electrical contacts on the crystal surface by using conducting silver paste according to “sandwich” geometry. For this purpose, first electrode was attached on the front side of the sample using a little amount of silver paste. Then we attached the sample to the top of a coin-like sample holder with the same paste. The second electrode is connected to the cryostat to make a close circuit. The electrons/holes stream within the sample in a sense along the *c*-axis in this configuration. A schematic diagram of the sandwich geometry is shown in the figure 3.1. The conductivity of the studied crystals within the layer is about four orders of magnitude higher than that normal to the layer [3]. Therefore, the distribution of electric field lines through the sample covers almost all the volume for the current contact configuration.

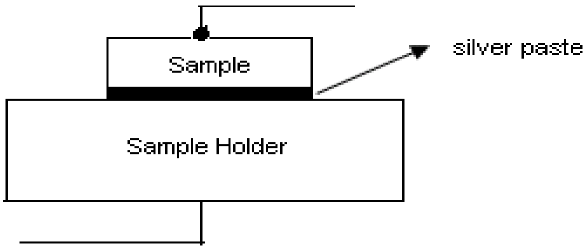

Fig. 3.1. The simple presentation of the sample with sandwich configuration.

3.4.3 Thermally Stimulated Current Measurements

The TSC measurements were performed in the temperature range from 10 to 300 K using the Advanced Research Systems closed-cycle helium cryostat. Constant heating rates ranges between 0.6–1.2 K s^{-1} were consummated using the temperature controller "Lake-Shore 331". A Keithley 228A voltage/current source and a Keithley 6485 picoammeter were used in the Thermally Stimulated Current experiments. The temperature sensitivity was about 10 mK and the current sensitivity was 2 pA in the used instruments. The view of the TSC experimental set up is shown in the figure 3.2.

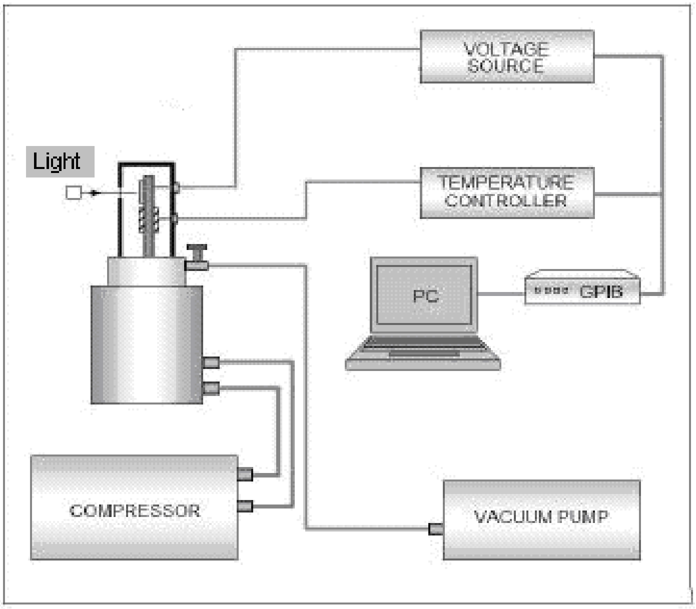

Fig. 3.2. Schematic diagram of the TSC experimental set up [44].

When the probability of trapped carriers to be released is insignificat; at initial low temperature, the electrons/holes are photo excited by a suitable LED generating radiation at a maximum intensity of 2.6 eV.

Both charge carriers hole and electron traps in TlGaSeS layered single crystals were studied. The investigation of hole traps were performed in temperature range from 10 to 100 K. The hole traps filling was performed by illumination under bias voltage of $V_1 = 1$ V at the initial temperature $T_0 =$ 10 K for about 10 min. Then the excitation was turned off. After waiting for ≈ 60 s as an expectation time a bias of V_2 was applied to the crystal and temperature was raised at constant heating rate. For TlGaSeS; a bias voltage of $V_2 = 100$ V can be applied while increasing the temperature heating since the dark current contribution is negligible.

The details of illumination time, voltage and initial temperature for TSC measurements for TlGaSeS crystals are recorded in the figure 3.3.

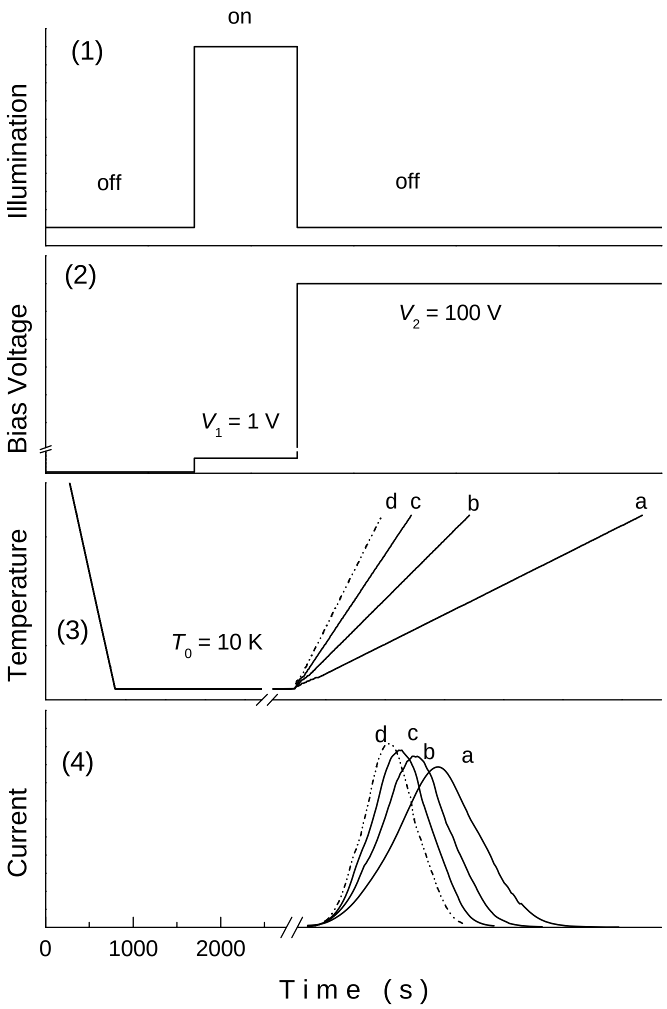

Fig. 3.3. Experimental condition of TSC measurements of TlGaSeS crystal in low temperature range. (1) time period of applied illumination; (2) variation of bias voltage; (3) temperature variation with time; (4) TSC peaks for different heating rates in K s^{-1}: 0.6 (a), 0.8 (b), 1.0 (c), 1.2 (d).

The investigation of electron traps were performed in temperature range from 10 to 160 K using the same set-up used for the investigation of hole traps. Here, a constant heating rates range of 0.6−1.2 K s^{-1} were used. The trap filling was performed by illumination under bias voltage of V_1 = 1 V at initial temperature T_0 =10 K for about 10 min. Then the illumination was set off. After waiting for about(≈ 60 s), we applied a voltage of V_2 to the crystal and temperature was raised at constant heating rate. Again a voltage of V_2 =100 V was applied during heating since as stated before, the dark current contribution is low in TlGaSeS crystals.

3.5 Photoconductivity Decay Experiments

Photoconductivity gain for different samples can be determined using various approaches. For this work, the following approach was used to determine *G* by utilizing photoconductivity decay experiment [45,46]. Using the photoconductivity decay experiments, the free charge carrier life time can be determined. The experiments are carried out by developing the following set-up. Ohmic contacts were performed on both sides of the sample according to sandwich geometry. The sample was irradiated using a LED “blue” controlled by a digital signal generator operating square waves “NI USB-6211 high-performance USB data acquisition device”. The photocurrent was amplified by a fast-current-voltage converter circuit. The signal was recorded by a fast digital voltmeter and transmitted to the computer and then treated to determine the photocurrent decay time. The schematic block diagram of the photoconductivity decay experimental set up is shown in the figure 3.4.

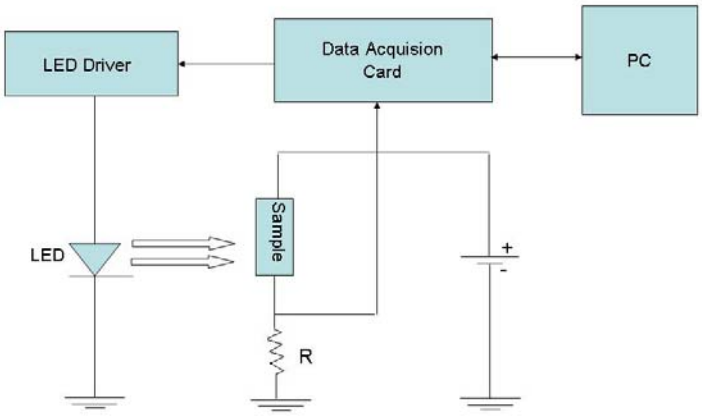

Fig. 3.4. The diagram of the photoconductivity experimental setup.

For the fact that current decays exponentially after light pulse is set off at $t = t_0$, the carrier lifetime τ is obtained by the corresponding output voltage relation, given by:

$$V = V_0 + C\exp(-t/\tau) \tag{3.1}$$

here, V_0 is the voltage at $t = \infty$ and C is a constant.

CHAPTER 4

RESULTS AND DISCUSSION

4.1 Introduction

In this part, the parameters of monoclinic unit cell will be found by studying the results of the X-ray powder diffraction. The element composite of TlGaSeS crystals will be obtained by studying the results of EDSA. Some optical properties of TlGaSeS crystals will be reported after analyzing the results of transmission and reflection measurements. The anaylsis of the results of the Thermally Stimulated Current experiments will be given to express the defect centers for both types of carriers in the crystal and their properties.

4.2 Results and Discussion of Energy Dispersive Spectroscopic and X-ray Experiments

The chemical composition of TlGaSeS crystals, shown in figure 4.1 was determined from energy dispersive spectroscopic analysis by using a JSM-6400 electron microscope. The composition of the studied crystal (Tl : Ga : S : Se) was found to be 25.7 : 25.9 : 24.1 : 24.3 . Moreover, EDSA indicated that silicon impurities were present in TlGaSeS.

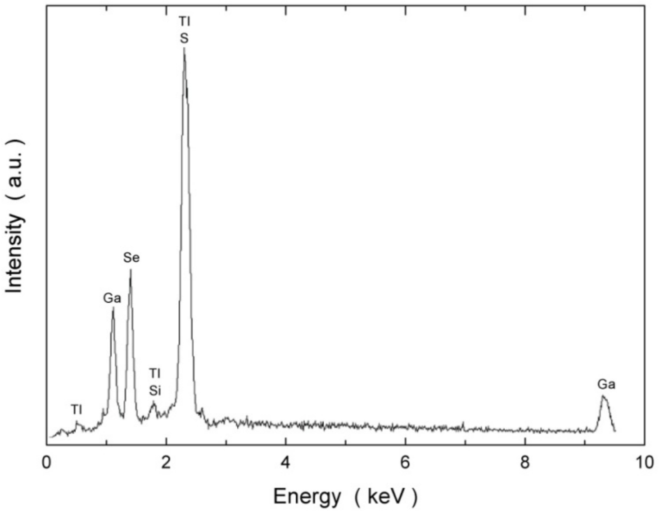

Fig. 4.1. Energy dispersive spectroscopic analysis of a TlGaSeS crystal.

The parameters of the monoclinic unit cell were found by performing the X-ray powder diffraction experiment. Figure 4.2 shows the X-ray diffractogram of the TlGaSeS layered crystal. The observed and calculated interplanar spacing (d), the miller indices ($h\ k\ l$), and the relative intensities (I/I_0) of the diffraction lines are given in Table 4.1. The lattice parameters of the monoclinic unit cell, calculated by using least-squares computer program “DICVOL 04”, were estimated to be $a = 0.7588, b = 0.7645, c = 0.8714$ nm and $\beta = 111.85°$.

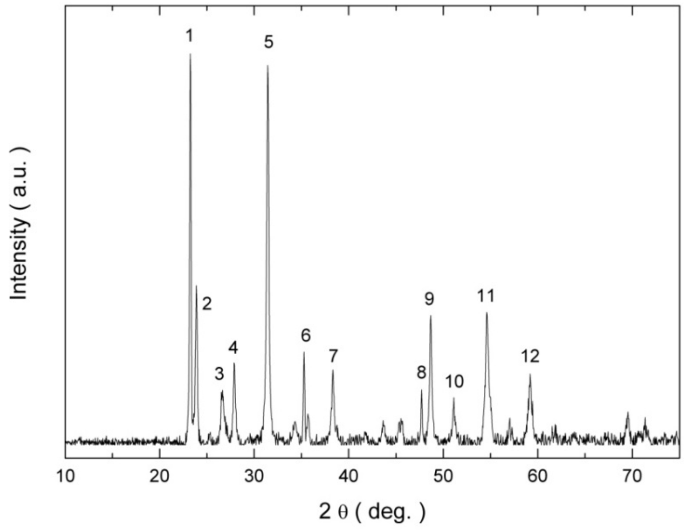

Fig. 4.2. X-ray diffraction pattern of a TlGaSeS powder sample.

Table 4.1. X-ray powder diffraction data for TlGaSeS crystals.

No.	$h\ k\ l$	d_{obs} (nm)	d_{calc} (nm)	I / I_0
1	0 2 0	0.3824	0.3823	100
2	2 1 –1	0.3723	0.3720	40.7
3	2 0 –2	0.3343	0.3343	14.0
4	0 1 2	0.3197	0.3199	21.0
5	2 2 –1	0.2843	0.2845	97.0
6	3 1 0	0.2542	0.2543	23.8
7	0 0 3	0.2347	0.2348	19.2
8	1 3 2	0.1904	0.1903	14.1
9	4 1 –3	0.1869	0.1869	33.1
10	3 1 2	0.1785	0.1785	12.1
11	0 4 2	0.1680	0.1680	33.9
12	3 4 0	0.1560	0.1559	18.2

4.3 Results and Discussion of Reflection and Transmission Experiments

The transmission (T) and reflectivity (R) spectra for TlGaSeS single crystal were obtained in the wavelength (λ) range of $400-1100$ nm (figure 4.3). The reflectivity and transmission of material are given by equations 2.7 and 2.9, respectively.

The absorption coefficient, α, is related to the absorption index k by

$$\alpha = \frac{4\pi k}{\lambda} \tag{4.1}$$

The reflectivity and the transmission measurements provided a determination of n, k, and α.

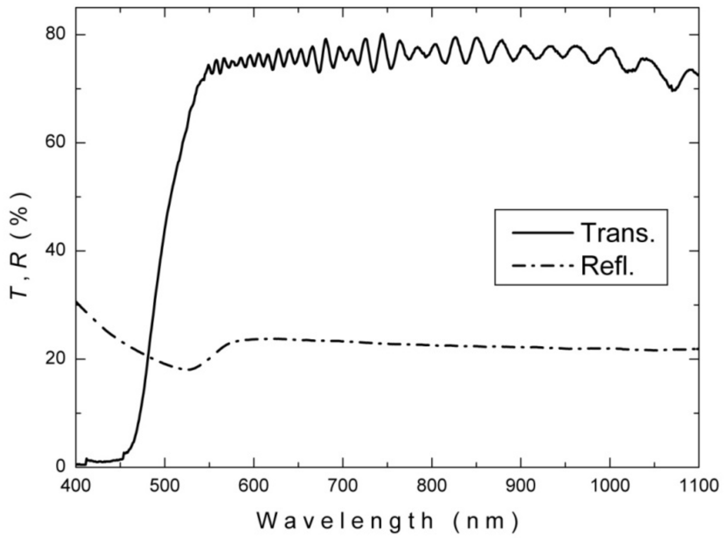

Fig. 4.3. Spectral dependence of the transmission and the reflectivity for a TlGaSeS crystal at $T = 300$ K.

The reflectivity is appraised using specimen with natural cleavage planes and a thickness satisfying "$\alpha d \gg 1$". The latter is determined by transmission measurements where an adhesive tape was used to fix the crystal to be suitable for the measurements. Using the obtained transmission interference fringes; the thickness was determined; at a wavelength slightly longer than the intrinsic absorption edge which corresponds to a relatively high transmission region (figure 4.3). The long-wavelength value of the refractive index $n = 2.72$, obtained from the reflection measurements, was used. For the room-temperature transmission measurements, the thickness of the sample was about 10 μm.

In order to obtain detailed information about the energy band gaps, we studied the dependence of the absorption coefficient on photon energy in absorption regions. The relation between the absorption coefficient α and the photon energy is given by relation 2.6

Figure 4.4, shows the absorption coefficient, α, calculated at room temperature for a TlGaSeS crystal in the photon energy range of 2.33−2.73 eV. It can be seen from figure 4.4 that as the photon energy increased from 2.33 to 2.73 eV, α changed from 27 to 3140 cm^{-1}. The analysis reveals that the α is proportional to $\left(h\nu - E_{\mathrm{g}}\right)^{\mathrm{p}}$with $p = 2$ and $p = 1/2$ for the energy ranges 2.33−2.52 eV and 2.58−2.73 eV, respectively. Insets of figure 4.4 shows the dependencies of $(\alpha h\nu)^{1/2}$ (inset 1) and $(\alpha h\nu)^2$ on the photon energy $h\nu$. In this figure, circles represent the experimental data; the solid lines are the linear fit which is used to find the band gaps. By extrapolating these fitted lines down to $(\alpha h\nu)^{1/2} = 0$ and $(\alpha h\nu)^2 = 0$, we obtained the values of the indirect band gap as $E_{\mathrm{gi}} = 2.27 \pm 0.02$ eV and the direct band as $E_{\mathrm{gd}} = 2.58 \pm 0.02$ eV. Worth to mention, the linear dependencies of $(\alpha h\nu)^{1/2}$ and $(\alpha h\nu)^2$ on the photon energy $h\nu$ suggest that indirect allowed transitions occurred in the range of 2.33−2.52 eV and direct transitions occurred in the intervals of 2.58−2.73 eV for the studied TlGaSeS.

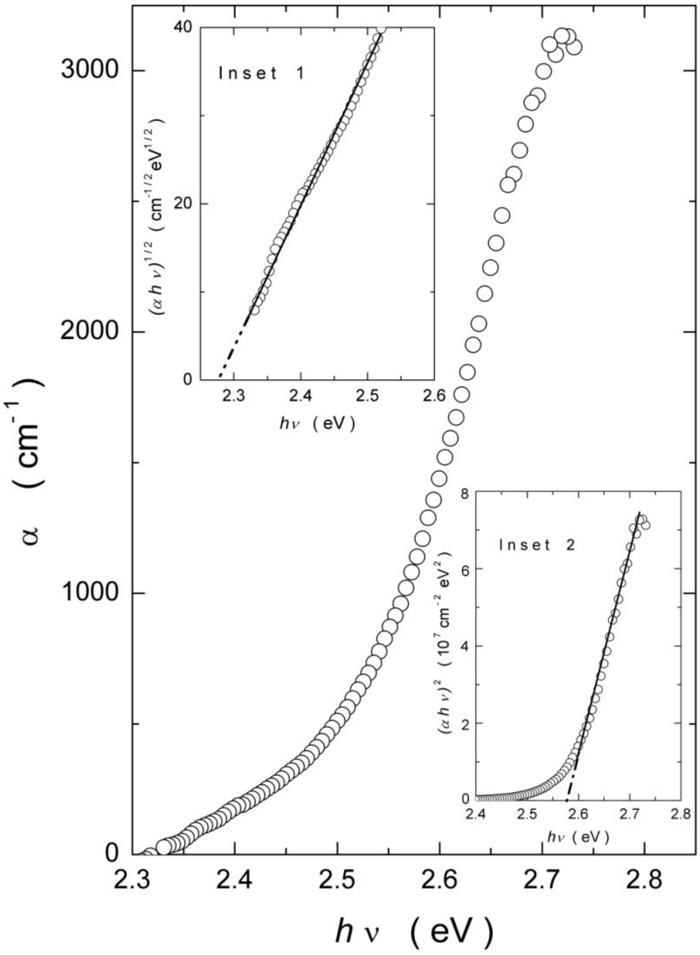

Fig. 4.4. Variation of the absorption coefficients as a function of photon energy at $T = 300$ K. Insets 1 and 2 represent the dependencies of $(\alpha h\nu)^{1/2}$ and $(\alpha h\nu)^2$ on photon energy, respectively.

Figure 4.5 shows the transmission spectra for a TlGaSeS layered single crystals being measured in the temperature range of 10−300 K. Thin layered crystals breaks into pieces at relatively low temperatures due to their high fragility. Therefore, the low-temperature measurements were done using thick samples, of thickness 300 μm. Consequently, we could analyze only the indirect energy band gap (E_{gi}) temperature dependence. Due to technical obstacles, we could not perform a direct measurements of low temperature reflectivity. Hence, to calculate the absorption coefficiet α, the spectral dependence of the room temperature reflectivity was shifted uniformly with energy according to the blue shift of the absorption edge.

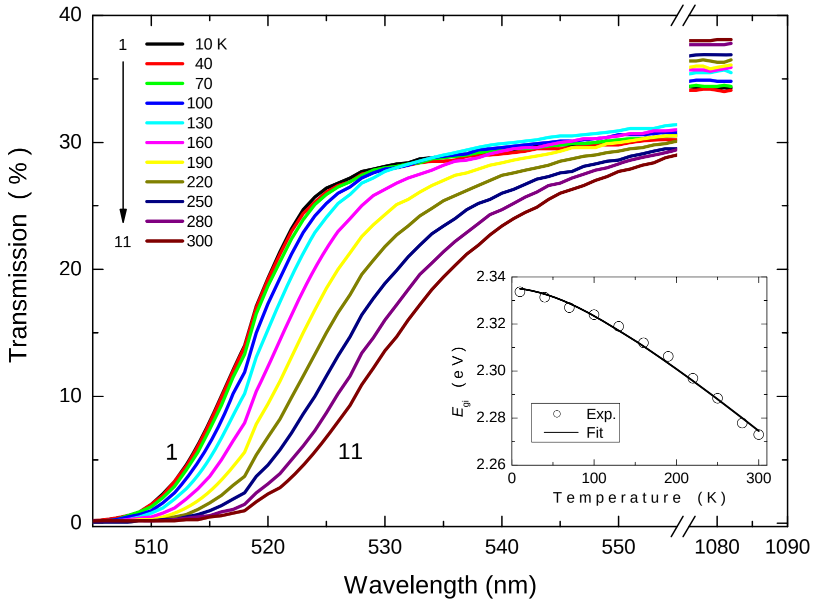

Fig. 4.5. Spectral dependence of the transmssion for TlGaSeS crystal in the temperature range of 10 − 300 K. Inset: The indirect band gap energy as a function of temperature. The solid line represents the fit using equation 4.5.

The indirect energy gap decreases with increasing temperature as it is shown from the inset of figure 4.5. That is, as the temperature increases from 10 to 300 K, it shifts from 2.33 to 2.27 eV. The temperature dependence of the energy band gap is given by the following relation [29]

$$E_{gi}(T) = E_{gi}(0) + \frac{\gamma T^2}{T+\beta} \quad , \tag{4.5}$$

where, $E_{\mathrm{gi}}(0)$ is the absolute zero value of the band gap, $\gamma = \mathrm{d}E_{\mathrm{gi}} / \mathrm{d}T$ is the rate of change of the indirect band gap with temperature, and β is approximately the Debye temperature. The data for the dependencies of E_{gi} on the temperature (10−300 K) were fitted using equation 4.5 as shown in the inset of figure 4.5 (the solid line correspond to the theoretical fit). From the fitting, the following parameters were found to be $E_{\mathrm{gi}}(0) = 2.34$ eV, $\gamma = -3.2\times10^{-4}$ eV/K, and $\beta = 165$ K for TlGaSeS crystals. The Debye temperature for the TlGaSeS crystals was estimated to be $\beta = 165$ K by using Lindemann's meltingrule [47] with X-ray results; as reported in the section 4.3, and the melting temperature $T_{\mathrm{m}} = 1135$ K.

The refractive index n was calculated using equations (4.1) and (4.2) as a function of wavelength and is shown in figure 4.6. The refractive index in the energy region of $h\nu < E_{\mathrm{g}}$ gradually decreases from 2.90 to 2.72 with increasing wavelength in the interval of 620−1100 nm, as seen in figure 4.6. The long wave-length value if the refractive index agrees with values of 2.6 ($\lambda = 1100$ nm) and 2.9 ($\lambda = 1500$ nm) reported for $TlGaS_2$ [48] and $TlGaSe_2$ [11] layered single crystals, respectively.

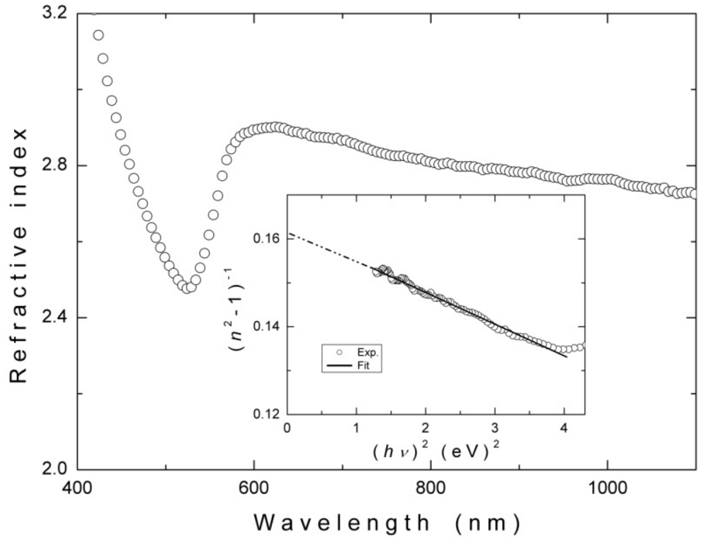

Fig. 4.6. Dependence of the refractive index on the wavelength for a TlGaSeS crystal. Inset: Plot on $(n^2 - 1)^{-1}$ versus $(h\nu)^2$. The solid line represents the fit using equation 4.6.

The dispersive refractive index was analyzed by means of single-effective-oscillator model. Previously, this model was successfully applied to the experimental data for ternary $TlGaS_2$ and $TlGaSe_2$ crystals [11,48]. Thus n can be expressed in terms of the photon energy, the single oscillator energy, E_{so} and the dispersion energy, E_{d}, by relation 2.1 .

Plotting $(n^2 - 1)^{-1}$ versus $(h\nu)^2$ allows the determination of the oscillator parameters by fitting a linear function to the lower energy data range 1.13−1.96 eV. The fits of the above reported function is presented in the inset of figure 4.6. The zero-frequency refractive index is obtained using relation 4.6, i.e. according to the expression $n_0^2 = 1 + E_{\mathrm{d}}/E_0$.

The value of E_{so} was obtained as 4.66 eV and the value of E_{d} was obtained as 24.28 eV by using the slope and the y-axis intersection with of the straight line (inset of figure 4.6). Furthermore, zero-frequency dielectric constant was determined as $\varepsilon_0 = n_0^2 = 7.15$ and zero-frequency refractive index $n_0 = 2.67$ were evaluated by means of equation 4.6. The oscillator energy E_{so} is an "average" energy gap and is approximately equal to two times the lowest direct band gap $E_{\mathrm{gd}}\left(E_{\mathrm{so}} \approx E_{\mathrm{gd}}\right)$ [32,49–53]. In this study, the ratio $E_{\mathrm{so}}/E_{\mathrm{gd}} = 1.83$ is found for TlGaSeS crystal.

4.4 Results and Discussion of Thermally Stimulated Current (TSC) Experiments

TSC measurements were carried out in as-grown TlGaSeS layered single crystals. The investigations for both hole and electron traps were performed. When the sample is illuminated at initial low temperature, both the electrons and holes are created in this region. Each of them can be driven out by the application of bias voltage causing different charge distribution in the crystal that is affected by the type of the trapping centres. To determine the type of the trap, we fill it by photo-excitation through different contacts. In our experiments, the samples were illuminated through the positive contact and the negative one as well. In this case, both hole and electron traps are distributed in the crystal and then trapped. Hence, the results for TSC on as-grown will be reported in two distinct sections each for one type of traps. Worth to mention, there are various methods to appraise the parameters of traps from the obtained TSC curve. We have used the different heating rates, curve fitting, initial rise, isothermal decay and trap distribution methods for the analysis of the data.

4.4.1 Results of TSC Observation of Hole Trapping Centres and their Distribution in as-grown TlGaSeS

4.4.1.1 Determination of the Trap Type and Minimum Excitation Time

When the sample was illuminated from the both contacts, the maximum Thermally Stimulated Current measured were equal 22.4 and 4.2 μA, respectively. The maximum of the peak is highest for the positive contact being illuminated rather than the negative one. This occurs when mainly the holes are distributed in the crystal and then trapped by hole trapping centres. Therefore the maximum appeared in TSC curve was assigned to hole traps.

It is useful to know the minimum illumination time necessary for carrying out TSC measurements. To fix this, the sample was illuminated for different time periods ranges between 50 and 900 s and the TSC curves in the temperature range of $10-100$ K were obtained at constant heating rate of $\beta = 0.8$ K s^{-1}. It is found that minimum illumination time is 600 s by plotting the maximum values of Thermally Stimulated Current ($I_{\max}$) versus excitation time as shown in figure 4.7 and 4.8.

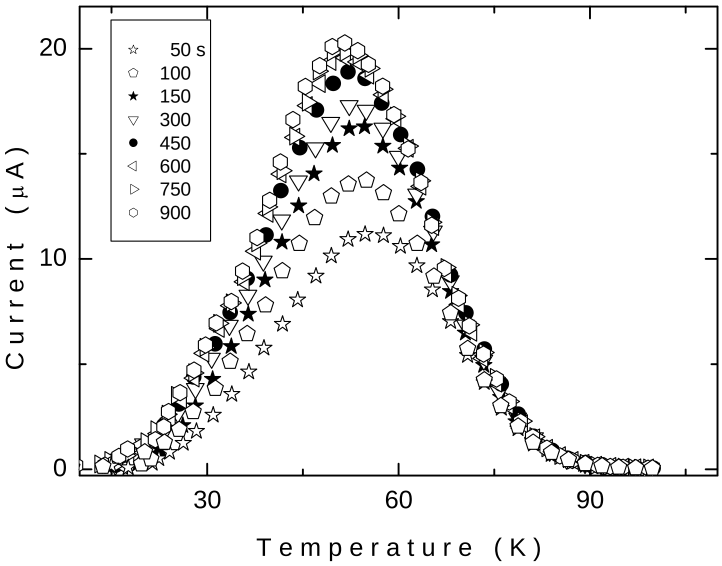

Fig. 4.7. TSC spectra of TlGaSeS crystal for various illumination times and a heating rate $\beta = 1\ \mathrm{K\ s^{-1}}$.

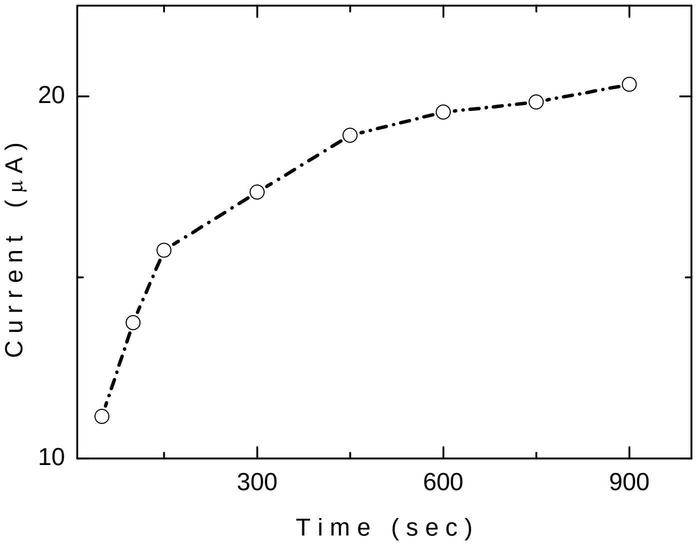

Fig. 4.8. The dependence of the maximum peak current on illumination time. The dash-dotted line is only guide for the eye.

4.4.1.2 Activation Energy Determination

Various methods to determine the activation energy of the trap can be used. Different heating rate, curve fitting, initial rise, isothermal and peak shape methods were used.

4.4.1.2.1 Different Heating Rate Method

Figure 4.9 represents typical TSC spectra of TlGaSeS single crystals measured for four linear heating rates of $\beta = 0.6$, 0.8, 1.0, and 1.2 K s^{-1} in the $10-100$ K temperature range. The TSC increases and the temperature at which the maximum value occurs shifts to a high temperature by increasing β. The activation energy E_t = 9 meV and the attempt-to-escape frequency $\nu = 0.51$ s^{-1} of trapped carrier were determined using the plot of $\ln(T_m^2/\beta)$ versus $(1/T_m)$ as shown in the inset of figure 4.10. The advantage of this method is that the activation energy is independent of the kinetic processes occurring in the studied crystals [19–22,35].

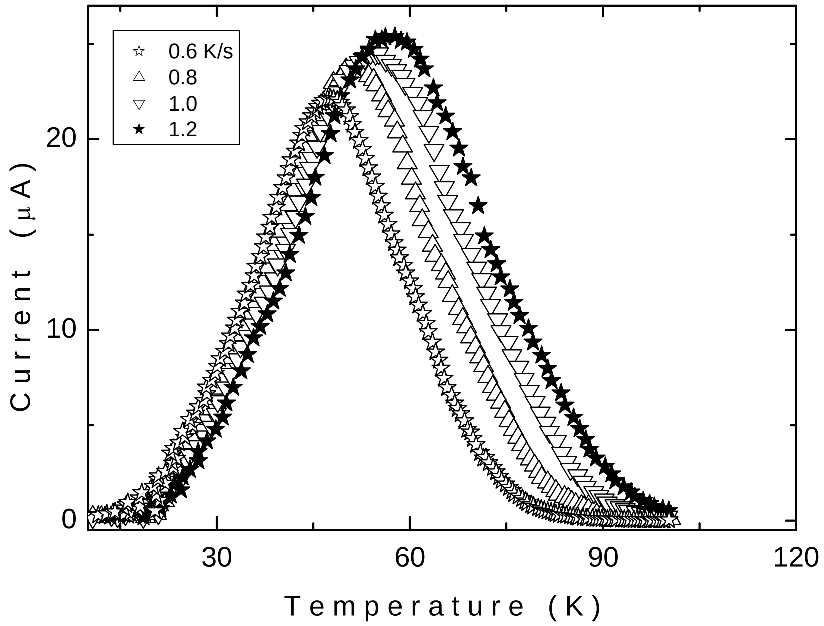

Fig. 4.9. Experimental TSC spectra of TlGaSeS crystals obtained with various heating rates.

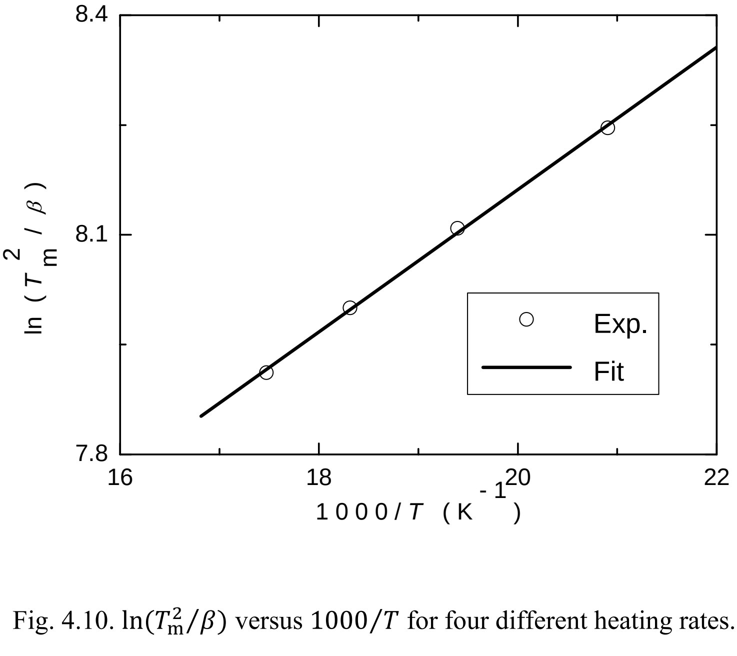

Fig. 4.10. $\ln(T_\mathrm{m}^2/\beta)$ versus $1000/T$ for four different heating rates.

4.4.1.2.2 Curve Fitting Method

Figure 4.11 shows the experimental TSC curve of the TlGaSeS for the heating rate of 0.8 K s^{-1}. From curve fit using equations 2.34 and 2.35 the activation energy is determined to be $E_t = 12$ meV and the attempt to escape frequency as $\nu = 0.57$ s^{-1}. A good agreement has been observed between the experimental TSC spectra and the theoretical one estimated with the assumption slow re-trapping. This suggests that re-trapping does not occur for the trapping centres of TlGaSeS crystals.

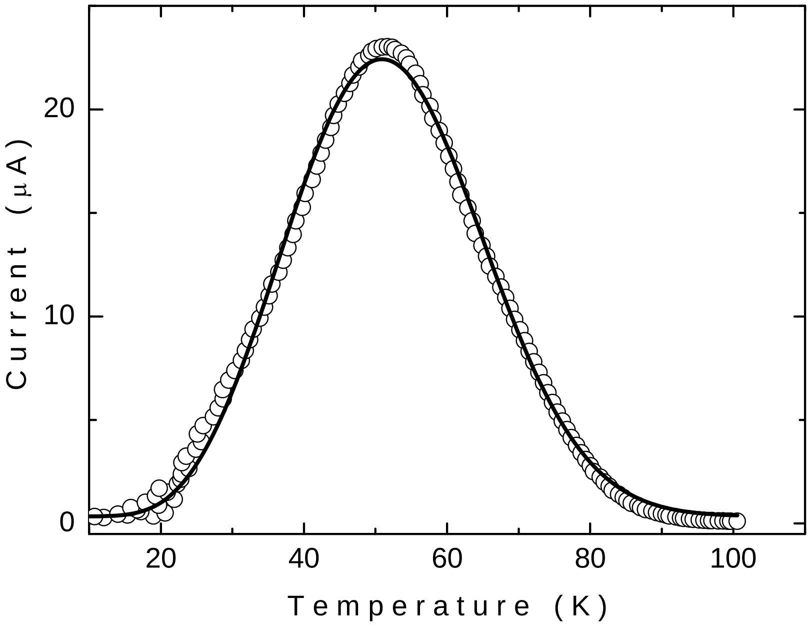

Fig. 4.11. TSC spectrum of TlGaSeS crystals with a heating rate of 0.8 K s^{-1}. Open circles are experimental data. Solid curve shows the fit to the experimental data.

4.4.1.2.3 Initial Rise Method

This method is valid for all types of recombination kinetics [19]. It is based on the assumption that the Thermally Stimulated Current is proportional to $\exp(-E_t/k)$ when the traps start to empty upon heating. The semi-logarithmic plot of the TSC versus $1/T$ gives a straight line whose slope is $(-E_t/k)$ as shown in figure 4.12. The activation energy is presented in Table 4.2.

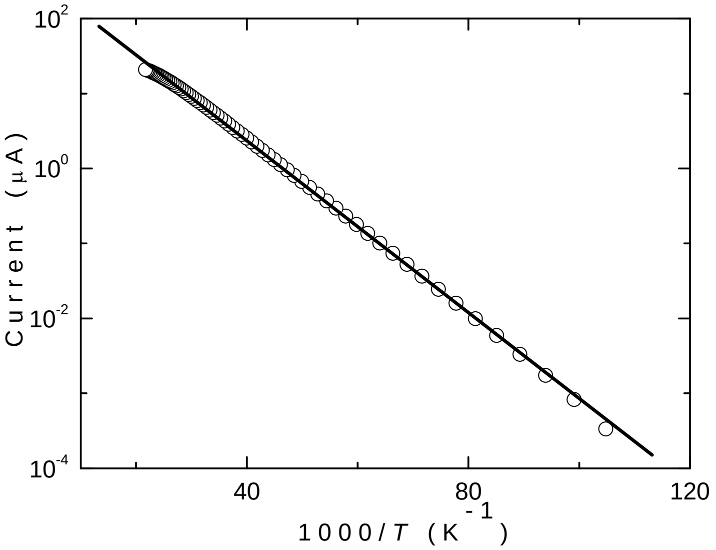

Fig. 4.12. TSC versus $1000/T$ for peak in the TSC spectrum of TlGaSeS crystals. Open circles are experimental data. Solid line is theoretical fit using initial rise method.

Table 4.2. The activation energy (E_t), capture cross section (S_t), attempt-to-escape frequency (v) and concentration (N_t) of hole traps for TSC peak of TlGaSeS crystal.

T_{max} (K)	E_t (meV)				S_t (cm^2)	v (s^{-1})	N_t (cm^{-3})
	Different heating rates method	Curve fitting method	Initial rise method	Isothermal decay method			
50.9	9	12	11	10	8.9×10^{-26}	0.51	7.7×10^{13}

4.4.1.2.4 Isothermal Method

In isothermal method, the sample is heated at constant rate from T_0 to T_p and then held at T_p until complete de-trapping. For this processes, the TSC can be described by equations 2.53 and 2.54. The TSC decay measurements on the TlGaSeS crystals were repeated at temperatures T_p = 24, 29, 34, 39, 46, and 51 K (figure 4.13). Thus, a series of slopes; i.e. γ −values of the plots $\ln(I)$ versus time t are obtained for each temperature T_p (figure 4.13). The ln values of the slopes versus $1/T_p$ of the figure 4.14 give a straight line from which E_t was obtained as 10 meV. The linear intersection of the $\ln(\gamma)$ versus $1/T_p$ graph gives the attempt-to-escape frequency $\nu = 0.73$ s^{-1}.

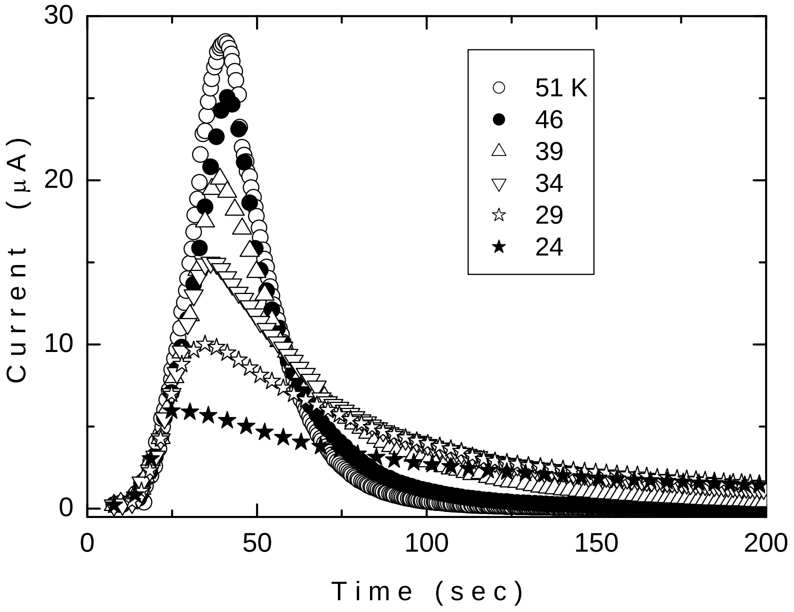

Fig. 4.13. Experimental TSC spectra of TlGaSeS crystals at different temperatures T_p.

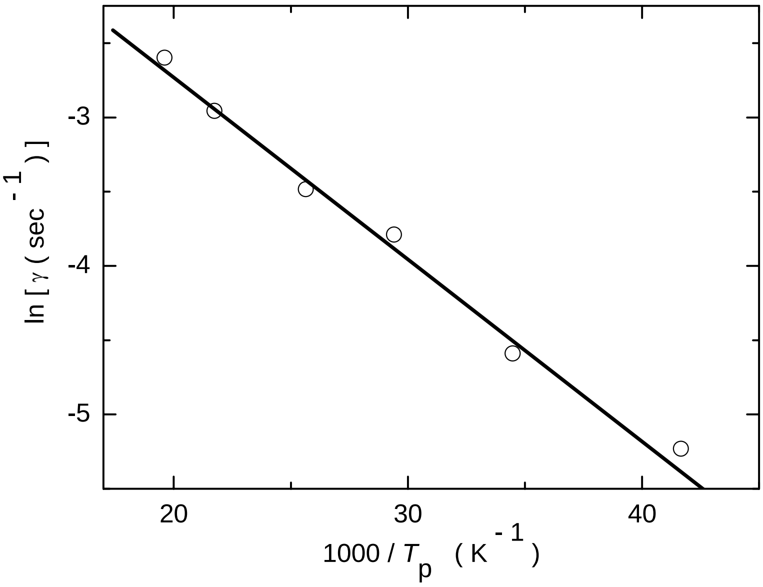

Fig. 4.14. ln(γ) plot as a function of $1/T_\text{p}$. Open circles are experimental data. The solid line is the linear fit to the experimental data.

4.4.1.2.5 Peak Shape Method

In peak shape method, T_{max} , T_{l} , and T_{h} of equations in section 2.7.6 were found to be 51.0, 35,3, and 67.5 K, respectively. These values were used in equations 2.50, 2.51, and 2.52 to find E_{τ}, E_{δ} and E_{w}. The averaged value of obtained activation energies E_{τ}, E_{δ} and $\mathrm{E_w}$ for the peaks is E_{av} = 15.3 meV.

4.4.1.3 Determination of the Traps Distribution

The analysis of TSC data gives information about the characteristic features of traps distribution. In this regard, the crystal was illuminated at different excitation temperatures T_0 ranging from 20 to 40 K, so as to allow trapping of photo-produced holes. Then, the light source is set off; the sample is kept in darkness and cooled to 10 K. Thereafter, the sample is successively heated with a linear rate to excite the trapped holes into the valence band. The experimental TSC spectra of TlGaSeS crystals at different excitation temperatures ($T_0 = 20, 25, 27, 30, 35$ and 40 K) are shown in figure 4.15.

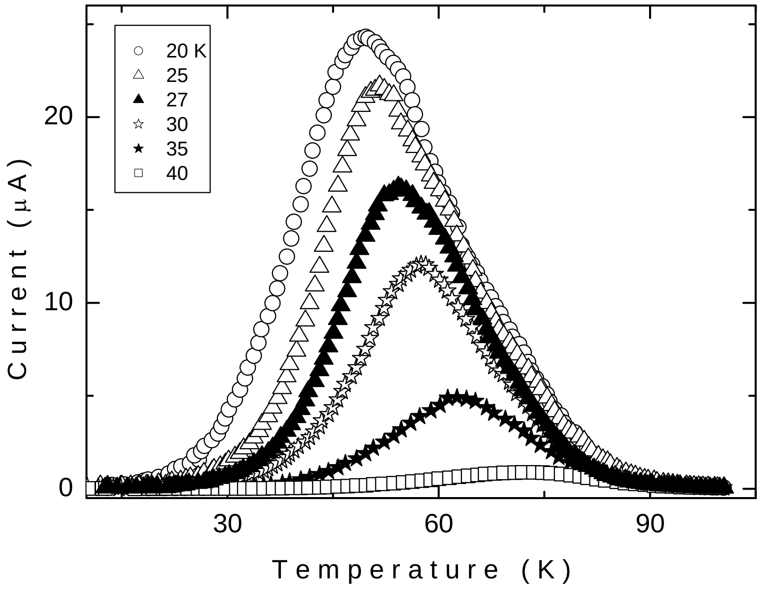

Fig. 4.15. Experimental TSC spectra of TlGaSeS crystals at different excitation temperatures T_0.

The TSC spectra decrease in intensity and shifts towards higher temperatures with increase in the light excitation temperature. This fact supports the validity of a quasi-continuous traps distribution [43,54–56]. The activation energies, determined by curve fitting method, and the maximum temperatures of thermo-current curves registered at different excitation temperatures are shown in Table 4.3. The activation energy ranges from 14 to 33 meV at T_0 = 20 and 40 K, respectively. It is observed that above T_0 = 40 K, the TSC spectra could not be analyzed due to their low intensity.

By assuming an exponential trap distribution, whose density at energy E_t given by equation 2.55, we can write equation 2.59. Figure 4.16 shows the plot of $\ln[S_0(I_m/I_e)]$ versus the activation energy E_t obtained by analyzing the TSC curves, which were recorded at different excitation temperatures. The obtained graph is a straight line which has a slope $\alpha_1 = 0.12$ meV^{-1} which corresponds to 18.9 meV/decade, an order of magnitude variation in the trap density for every 18.9 meV.

Table 4.3. TSC parameters for TlGaSeS crystals at different excitation temperatures.

Curve	1	2	3	4	5	6
Exication temperature (K)	20.0	25.0	27.0	30.0	35.0	40.0
Maximum temperature (K)	49.6	51.6	54.2	57.4	61.9	72.8
Curve area (au)	719	574	409	296	120	24
Activation energy (meV)	14	18	21	24	29	33

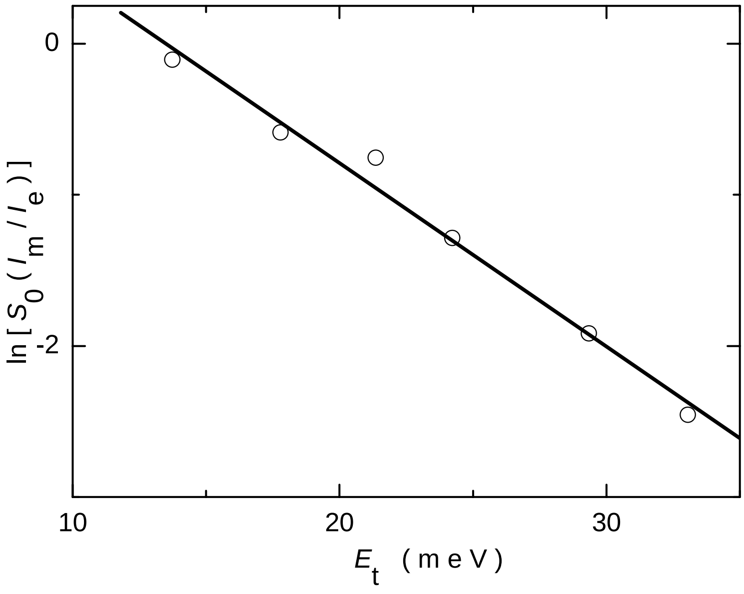

Fig. 4.16. $\ln[S_0(I_m/I_e)]$ plot as a function of activation energy E_t. Open circles are experimental data. Solid line is the linear fit to the experimental data.

4.4.1.4 Determination of Capture Cross-Section and Concentration of the Traps

Once the TSC was fitted and the values of E_t and T_m were obtained (Table 4.3), equations 2.35 and 2.40 were used to obtain B and ν; the attempt-to-escape frequency. Using the value of $\nu = 0.57$ s^{-1}, the capture cross-section area of traps was evaluated using equation 2.46, where the effective density of states in the valence band and the thermal velocity of free hole are used to study the hole traps. The calculated value of S_t was found to be 8.9×10^{-26} cm^2. The small value of the capture cross-section justifies the assumption of monomolecular kinetics.

The traps concentration was obtained with the use of equation 2.47. The dimensions of the sample $9\times1\times0.8$ mm^3 were used. The photoconductivity gain was measured by photoconductivity decay measurements in which equation 3.1 was used to evaluate the carrier lifetime τ; figure 4.17 is the theoretical fit to the experimental data in the light of equation 3.1. Using the value of $\tau = 2.3\times10^{-3}$ s in equation 2.48, the photoconductivity gain was found to be $G = 1096$ using $V_2 = 50$ V and $\mu = 61$ $cm^2V^{-1}s^{-1}$ [57]. The concentration of traps was found to be $N_t = 7.7\times10^{13}$ cm^{-3} using equation 2.47.

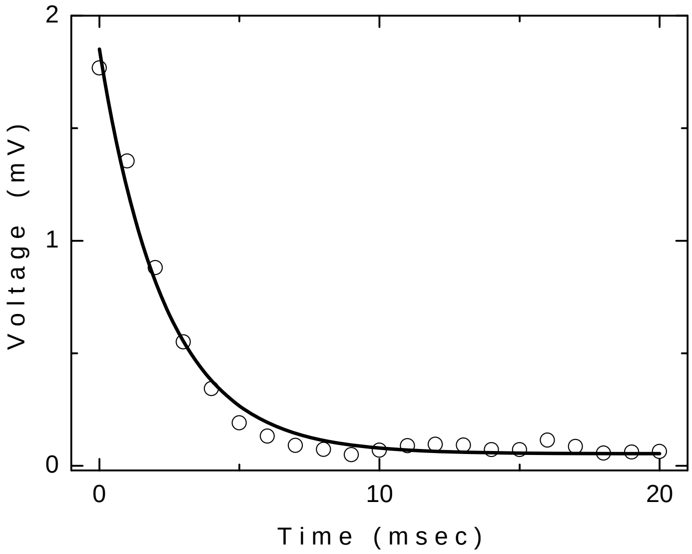

Fig. 4.17. A photoconductivity decay curve for TlGaSeS crystal. Open circles are experimental data. Solid curve shows the theoretical fit to the experimental data.

4.4.2 Results of TSC Observation of Electron Trapping Centres and their Distribution in as-grown TlGaSeS

4.4.2.1 Determination of the Trap Type and Minimum Excitation Time

In this part, the sample was illuminated through the negative contact. In this case, mainly the electrons are distributed in the crystal and then trapped. Therefore, the observed peaks in TSC spectra of TlGaSeS crystal are assigned to electrons traps as shown in figures 4.18 and 4.19.

Once again it is of great importance to fix the needed minimum illumination time to carry out the Thermally Stimulated Current measurements. To determine this, the same procedure used while analyzing hole traps was followed and the minimum illumination time was found as 600 s.

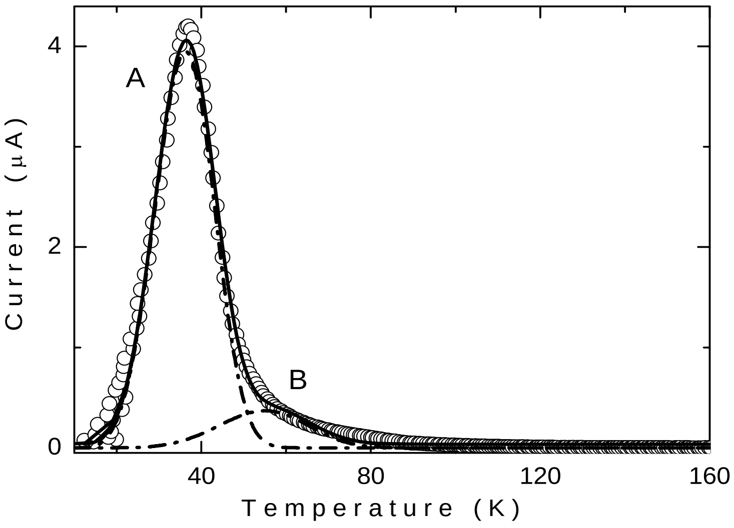

Fig. 4.18. Experimental TSC spectrum of TlGaSeS crystals registered at the excitation temperature $T_0 = 10$ K and decomposition of this spectrum into two peaks (A and B). Open circles are experimental data. Dashed curves represent decomposed peaks. Solid curve shows total fit to the experimental data.

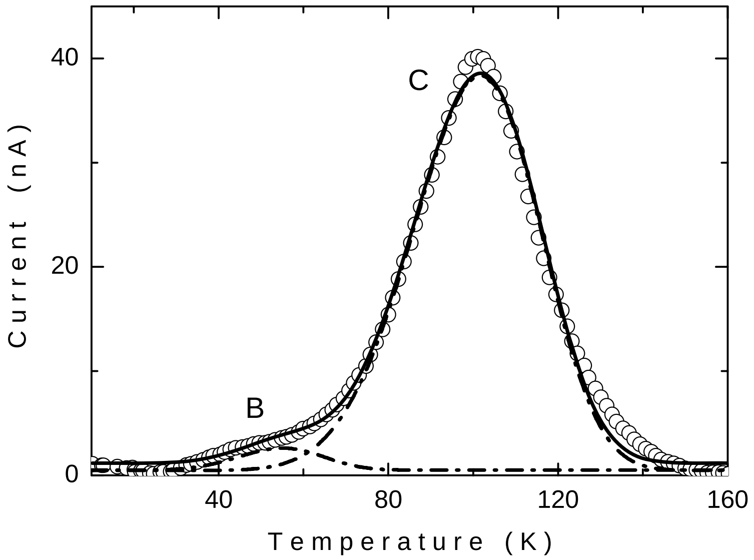

Fig. 4.19. Experimental TSC spectrum of TlGaSeS crystal obtained after the thermal cleaning at $T \approx 55$ K and decomposition of this spectrum into two separate peaks (B and C). Open circles are experimental data. Dashed curves represent decomposed peaks. Solid curve shows total fit to the experimental data.

4.4.2.2 Activation Energy Determination

Several methods to evaluate different parameters of the trapping centres can be used. The number of overlapping peaks restricts the applicability of some of these methods. To analyze the TSC spectra for electron trapping centres, curve fitting, initial rise, and peak shape methods were used.

4.4.2.2.1 Curve Fitting Method

This method is used for decomposition of the TSC spectra into separate peaks. For slow re-trapping which is knows as monomolecular conditions, Thermally Stimulated Current curve of a discrete set of traps with activation energy E_t is given by relations 2.28a, 2.34, 2.35, and 2.40. In order to analyze all peaks of spectra simultaneously, the fitting function which is given summing all features of the TSC spectra is given by 2.45.

Figure 4.18 shows the experimental TSC spectrum of TlGaSeS crystal obtained at the excitation temperature T_0 = 10 K using the heating rate of β =0.8 K s^{-1}. Attempts to fit the theoretical curve to measured data with only single peak failed. A fit of the data using two peaks (distinguished as A and B) was done and a result of an excellent fit for the measured spectra was obtained. The activation energies associated with these two peaks were found to be E_A = 12 meV and E_B = 20 meV. Thereafter, the so-called "thermal cleaning" technique was used to prove that there is an additional weak peaks in the high-temperature part of the spectra along with peaks A and B. "Thermal cleaning" process was done as follows: first we cooled the crystal and then illumination with suitable light source was applied at T_0 = 10 K. Then the same heating cycle as before was followed, this time we turned heating off at a temperature near T_{max} = 58 K of peak B. Consequently, the traps contributing for the TSC peaks given by A and B were substantially emptied. Then the sample was cooled down in the dark to T_0 = 10 K and heated again at the same heating rate. The quenching of the high-intensity peaks A and B has made it possible to observe the details of the other remaining part which is somehow smaller in intensity as shown in figure 4.19. However, the third peak C was not registered separately, due to the fact that peak B has much higher initial intensity (almost 10 times) than that peak C. A weak shoulder due peak B on the low temperature side of TSC curve was noticed. This can be illustrated by the fact that the impurity levels corresponding to peak B could not be emptied entirely. It could be possible to empty completely the trapping centres associated to the peak B by applying higher thermal cleaning temperatures. However, it was observed that such a process decreases the intensity of the third peak C drastically. The attempts to make fitting for the measured experimental spectra of thermally cleaned spectrum using only single peak failed either. Therefore, a fit of the observed spectrum using two peaks (B and C) was done successfully. The theoretical curve calculated for two peaks with activation energies E_B = 20 meV and E_c = 49 meV is compatible with the thermally cleaned experimental data in the $10-160$ K temperature range as shown in figure 4.18.

Fair enough agreement has been attained between the experimental TSC spectra and the theoretical ones, estimated by the assumption of slow re-trapping (fig. 4.18 and fig. 4.19). This suggests that there is no re-trapping for the trapping centres of the TlGaSeS crystal. The parameters of the three electrons trapping centres in TlGaSeS crystals were determined and reported in Table 4.4.

4.4.2.2.2 Initial Rise Method

Again as illustrated in section 4.4.1.2.3, a semi-logarithmic plot of the current versus $1/T$ gives a straight line which has a slope of $-E_t/\kappa$. The plots for TSC peaks of the studied sample are presented in figure 4.20. The activation energies of the traps calculated by this method are reported in Table 4.5

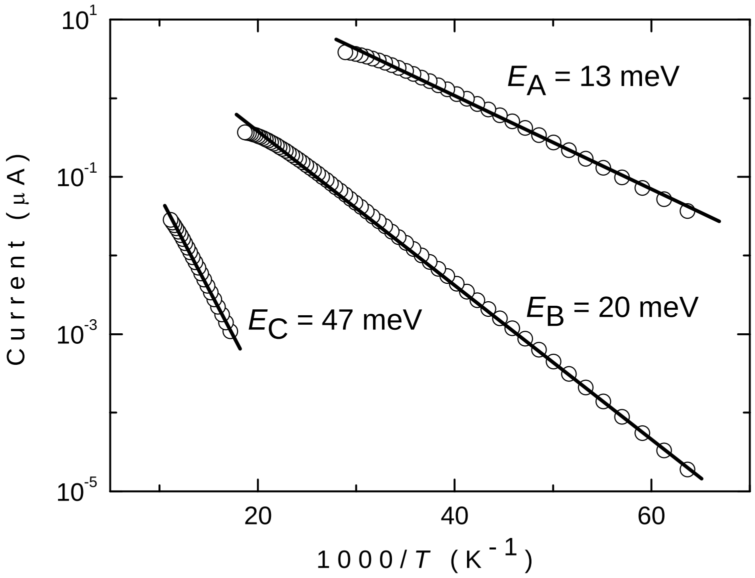

Fig. 4.20. TSC versus 1000/T for all three peaks in TSC spectra of TlGaSeS crystal. Open circles are experimental data. Solid lines show fits to the experimental data for A, B and C peaks.

Table 4.4. The activation energy (E_t), capture cross section (S_t), attempt-to-escape frequency (ν) and concentration (N_t) of electron traps for three TSC peaks of TlGaSeS crystal.

Peak	T_m (K)	E_t (meV)			ν (s^{-1})	S_t (cm^2)	N_t (cm^{-3})
		Curve fitting method	Chen method	Initial rise Method			
A	38.7	12	15	13	2.8	2.1×10^{-24}	2.0×10^{12}
B	58.0	20	23	20	3.1	1.0×10^{-24}	2.8×10^{11}
C	103.0	49	52	47	11.8	1.1×10^{-24}	4.4×10^{10}

4.4.1.2.3 Peak Shape Method

In peak shape method, T_m , T_l , and T_h of equations in section 2.7.6 were found to be 36.5, 27,6, and 44.4 K, respectively for peak A, 55.1, 42.3, and 66.6 K, respectively for peak B, and 101.7, 81.2, and 117.0, respectively for peak C. These values were used in equations 2.50, 2.51, and 2.52 for each peak to find E_τ, E_δ and E_w. The averaged value of obtained activation energies E_τ, E_δ and E_w for the peaks is E_{av} = 15, 23, and 52 meV for peaks A, B, and C respectively.

4.4.2.3 Determination of the Traps Distribution

The same procedure illustrated in section 4.4.1.3 was followed but in this case the crystal was excited by light at different illumination temperatures T_0 ranging from 20 to 31 K for peak A and from 57 to 70 K for peak C so as to allow trapping of photo-produced electrons. Then, the light source is turned off; the sample is kept in darkness and cooled to 10 K. Thereafter, the sample is successively heated with a constant linear heating rate $\beta = 0.8$ K s^{-1} to excite the trapped electrons into the conduction band.

Figures 4.21 and 4.22 show the experimental TSC spectra of TlGaSeS crystals obtained at different excitation temperatures (T_{0A} = 20, 23, 26, 29, and 31 K) for peak A and (T_{0C} = 55, 57, 60, and 70 K) for peak C.

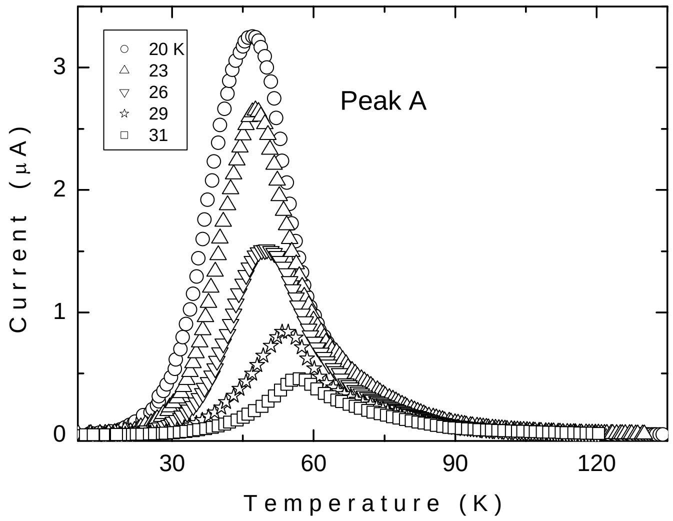

Fig. 4.21. Experimental TSC spectra (peak A) of TlGaSeS crystals at different excitation temperatures T_0.

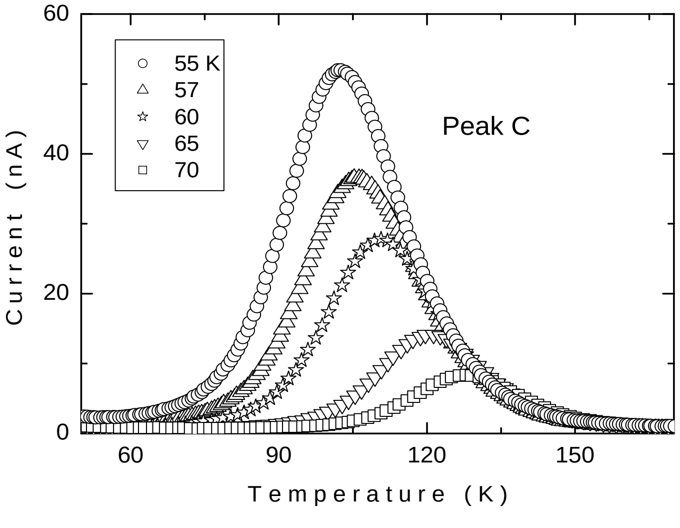

Fig. 4.22. Experimental TSC spectra (peak C) of TlGaSeS crystals at different excitation temperatures T_0.

Again, the TSC spectra decrease in intensity and shifts towards higher temperatures with increase in the light excitation temperature. This fact supports the validity of a quasi-continuous traps distribution [43,54–56]. The activation energies, found by curve fitting method, and the maximum temperatures of thermo-current curves registered at different excitation temperatures are reported in Table 4.5. The activation energies range from 18 to 25 meV at T_0 = 20 and 31, respectively for peak A, and from 66 to 122 meV at T_0 = 55 and 70 K, respectively for peak C. It is observed that above T_0 = 31 K (peak A) and T_0 = 70 K (peak C) the TSC spectra could not be analyzed due to their low intensity.

Similar to the procedure followed in section 4.5.1.3, by assuming an exponential trap distribution, whose density at energy E_{t} given by equation 2.55, we can write equation 2.59. Figures 4.23 and 4.24 show the $\ln[S_0(I_{\mathrm{m}}/I_{\mathrm{e}})]$ plotted as a function of the activation energy E_{t} obtained by analysing the TSC curves, which were recorded at different excitation temperatures. The obtained graph for peak A is a straight line which has a slope of $\alpha_1 = 0.26$ meV^{-1} which corresponds to 9 meV/decade, an order of magnitude variation in the trap density for every 9 meV. Similarly peak C, the straight line has a slope of $\alpha_1 = 0.028$ meV^{-1} which corresponds to 81 meV/decade, an order of magnitude variation in the trap density for every 81 meV.

Table 4.5. TSC parameters for TlGaSeS crystals for peaks A and C at different excitation temperatures.

	Peak A					Peak C				
Curve*	1	2	3	4	5	1	2	3	4	5
Excitation temperature (K)	20	23	26	29	31	55	57	60	65	70
Maximum temperature (K)	47.0	47.7	50.1	54.2	56.9	102.6	105.2	110.7	119.7	127.9
Curve area (a.u.)	78	60	37	21	12	1807	1249	944	499	325
Activation energy (meV)	18	20	21	23	25	66	73	81	106	122

*See Figs. 4.21 and 4.22.

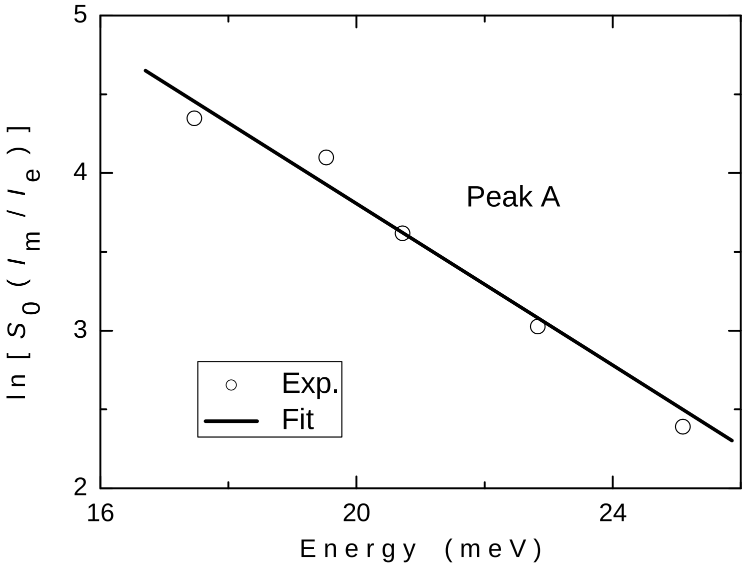

Fig. 4.23. $\ln[S_0(I_m/I_e)]$ plot as a function of activation energy E_t for peak A. Open circles are experimental data. Solid line is the linear fit to the experimental data.

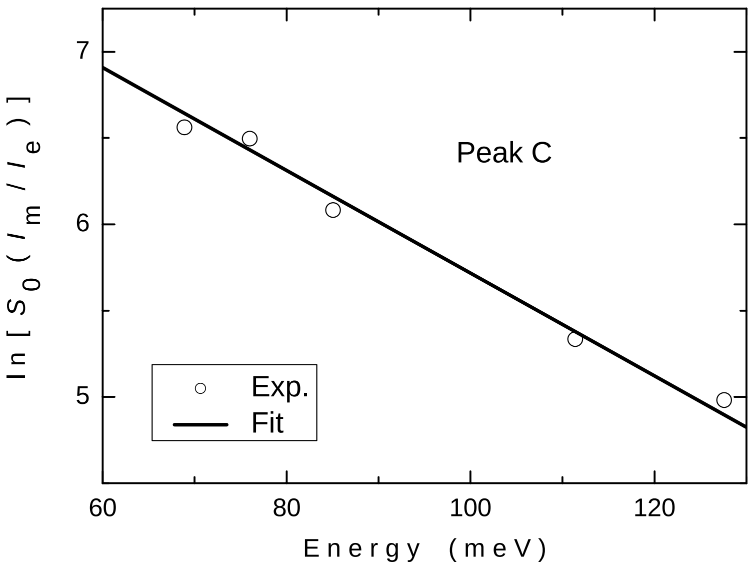

Fig. 4.24. $\ln[S_0(I_m/I_e)]$ plot as a function of activation energy E_t for peak C. Open circles are experimental data. Solid line is the linear fit to the experimental data.

4.4.2.4 Determination of Capture Cross-Section and Concentration of the Traps

The same discussion of section 4.4.1.4; once the TSC was fitted and the values of E_t and T_m were obtained (Table 4.4), equations 2.35 and 2.40 were used to calculate B and the attempt-to-escape frequency ν. Using the values of ν (Table 4.4), the capture cross-section area of traps was evaluated using equation 2.46, where the effective density of states in the conduction band and the thermal velocity of free electron are considered to study the electron traps. The calculated value of S_t was found to be 2.1×

10^{-24}, 1.0×10^{-24}, and 1.1×10^{-24} cm^2 for peaks A, B and C. The small value of the capture cross-section justifies the assumption of monomolecular kinetics.

The traps concentration was obtained with the use of equation 2.47. The dimensions of the sample $9\times1\times0.8$ mm^3 were used. The photoconductivity gain was measured by photoconductivity decay measurements in which equation 3.1 was used to evaluate the carrier lifetime τ; figure 4.25 shows the theoretical fit to the experimental data in the light of equation 3.1. Using the value of $\tau = 3.8\times10^{-2}$ s in equation 2.48 the photoconductivity gain was found to be G = 3622 using V_2 = 10 V and μ = 61 cm^{2}V^{-1}s^{-1} [57].The concentration of traps N_t (Table 4.4) was found to be 2.0×10^{12}, 2.8×10^{11}, and 4.4×10^{10} cm^{-3} for peaks A, B and C, respectively using equation 2.47.

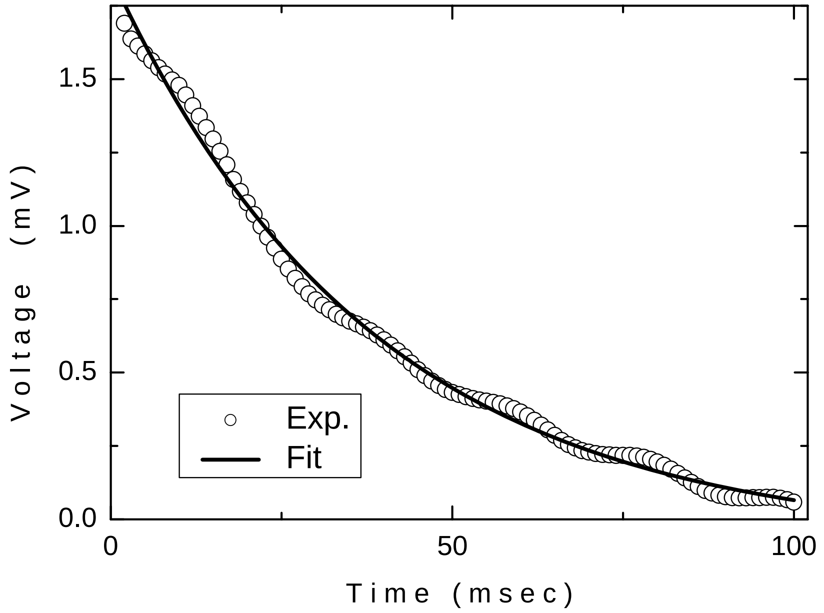

Fig. 4.25. The photoconductivity decay curve for the TlGaSeS crystal. Open circles are experimental data. Solid curve shows the theoretical fit to the experimental data.

CHAPTER 5

CONCLUSION

In this work, an X-ray powder diffraction analysis was used to characterize TlGaSeS crystals. The parameters associated with the monoclinic unit cell were estimated to be $a = 0.7588, b = 0.7645, c = 0.8714$ nm and $\beta = 111.85^{\circ}$. The absorption coefficient and the refractive index were determined by measuring the optical transmission and reflection of TlGaSeS crystals over the spectral region of 400–1100 nm. A coexistence of both transitions the indirect and the direct one in the studied TlGaSeS with energy band gaps of 2.27 and 2.58 eV. There values were observed as a result of the room-temperature absorption data analysis. The absorption edge was found to shift toward lower energy as we increase the temperature from 10 K up to 300 K. The temperature dependence of the indirect energy band gap of the crystal was determined as a function of tempeature. The rate of change on the indirect band gap with temperature was found to be $\gamma = -3.2\times 10^{-4}$eV/K. Moreover, the value of the absolute-zero band gap energy, $E_{\mathrm{gi}}(0)$, was determined as 2.34 eV. The Wemple-DiDomenico single-effective-oscillator model was used to analyze the refractive index dispersion data. As a result of this analysis, the dispersion energy and the zero-frequency refractive index were obtained.

A hole trapping centre with activation energy of 12 meV and three electron trapping centres with activation energies 12, 20, and 49 meV (for A-, B-, C-peaks, respectively) were obtained TlGaSeS layered single crystals using TSC measurement. The observed trapping levels are thought to originate from defects, created while growing the sample, and/or unintentional impurities due to the fact that samples used in these measurements are not intentionally doped. The traps parameters which were obtained by using several distinct methods of analysis agree with each other. The re-trapping process is negligible as assured by the good agreement between the experimental outcomes and the theoretical predictions of the model that assumes slow re-trapping.

For hole trapping centre, the capture cross-section and the concentration of the traps were calculated to be 8.9×10^{-26} cm^2 and 2.0×10^{14} cm^{-3}, respectively. The quasi-continuous distribution of the shallow hole traps in the studies crystals were revealed by the analysis of the TSC spectra. The variation on one order of magnitude in the trap density for every 18.9 meV was obtained.

Furthermore, for the electron trapping centres, the capture cross-section of the traps were calculated to be 2.1×10^{-24}, 1.0×10^{-24} and 1.1×10^{-24} cm^2. Furthermore, the concentrations of the traps were found to be 2.0×10^{12}, 2.8×10^{11} and 4.4×10^{10} cm^{-3}. Exponential distribution of electron trapping centres was also obtained by analysing the data recorded at different illumination temperatures. Using this measurement, values of 9 and 81 meV/decade for traps distribution of peaks A and C, respectively were obtained.

REFERENCES

[1] D. Müller and H. Hahn, *Z. Anorg. Allg. Chemie* **438**, 258 (1978).

[2] K. A. Yee and A. Albright, *J. Am. Chem. Soc*. **113**, 6474 (1991).

[3] M. Hanias, A. Anagnostopoulos, K. Kambas, and J. Spyridelis, *Mat. Res. Bull*. **27**, 25 (1992).

[4] I. M. Ashraf, M. M. Abdel-Rahman, and A. M. Badr, *J. Phys. D: Appl. Phys*. **36**, 109 (2003).

[5] A. Kato, M. Nishigaki, N. Mamedov, M. Yamazaki, S. Abdullaeva, E.Kerimova, H. Uchiki, and S. Iida, *J. Phys. Chem. Sol*. **64**, 1713 (2003).

[6] Y. Shim, W. Okada, and K. Wakita, *J. Appl. Phys*. **102**, 083537 (2007).

[7] S. Duman and B. Gurbuluk, *Phys. Scripta* **72**, 82 (2005).

[8] V. Grivickas, V. Bikbajevas, and P. Grivickas, *Phys. Stat. Sol. (b)* **243**, R31 (2006).

[9] K. R. Allakhverdiev, *Solid State Commun*. **111**, 253 (1999).

[10] N. M. Gasanly, A. F. Goncharov, N. N. Melnik, A. S. Ragimov, and V. I. Tagirov, *Phys. Stat. Sol. (b)* **116**, 427 (1983).

[11] M. M. El-Nahass, M. M. Sallam, S. A. Rahman, and E. M. Ibrahim, *Solid State Sci*. **8**, 488 (2006).

[12] B. Gurbuluk and S. Duman, *Phys. Scr*. **77**, 025702 (2008).

[13] O. Karabulut, M. Parlak, and G. M. Mamedov, *J. All. Comp*. **429**, 50 (2007).

[14] S. G. Abdullaeva and N. T. Mamedov, *Phys. Stat. Sol. (b)* **133**, 171 (1986).

[15] C. S. Yoon, B. H. Kim, D. J. Cha, and W. T Kim, *J. Appl. Phys*. **32**, 32 (1993).

[16] S. G. Abdullaeva, G. L. Belenkii, and N. T. Mamedov, *Phys. Stat. Sol*.

(b) **102**, K19 (1980).

[17] V. Grivickas, V. Bikbajevas, M. I. Tarasik, and A. K. Fedotov, *Lithuanian J. Phys*. **46**, 1 (2006).

[18] S. Kashida, Y. Yanadori, Y. Otaki, Y. Seki, and A. M. Panich, *Phys. Stat. Sol. (a)* **203**, 2666 (2006).

[19] R. Chen and S. W. S. McKeever, *Theory of Thermuliminescence and related Phenomena*, Word Scientific, Singapore (1997).

[20] R. Schmechel and H. von Seggern, *Phys. Stat. Sol. (a)* **201**, 1215 (2004).

[21] V. M. Skorikov, V. I. Chmyrev, V. V. Zuev, and E. V. Larina, *Inorg. Mater*. **38**, 751 (2002).

[22] R. Bube, *Photoelectronic Properties of Semiconductors*, Cambridge University Press, Cambridge (1992).

[23] J. T. Randall and M. H. F. Wilkins, *Proc. Roy. Soc. A* **184**, 390 (1945).

[24] R. R. Haering and E. N. Adams, *Phys. Rev.* **117**, 451 (1960).

[25] K. H. Nicholas and J. Woods, *Brit. J. Appl. Phys.* **15**, 783 (1964).

[26] G. A. Dussel and R. H. Bube, *Phys. Rev.* **155**, 764 (1967).

[27] C. Kittel, *Introduction to Solid State Physics,* Wiley, New York (1971).

[28] W. L. Bragg, *Proceedings of the Royal Society of London Series A* **17,** Part I, 43 (1913).

[29] J. I. Pankove, *Optical Processes in Semiconductors*, Prentice Hall, New Jersey (1971).

[30] T. S. Moss, G. J. Burrell, and B. Ellis, *Semiconductor Opto-Electronics*, John Wiley & Sons, New York (1973).

[31] S. H. Wemple and M. DiDomenico, *Phys. Rev. Lett.* **23**, 1156 (1969).

[32] K. Tanaka, *Thin Solid Films* **66**, 271 (1980).

[33] R. Chen and Y. Kirsh, *Analysis of Thermally Stimulated Processes*, Pergamon Press, Oxford (1981).

[34] S. W. S. McKeever, *Thermoluminescence of Solids*, Cambridge Uni. Press, Cambridge (1985).

[35] G. Kitis, R. Chen, and V. Pagonis, *Phys. Stat. Sol. (a)* **205**, 1181 (2008).

[36] M. Kumar, G. Chourasiya, B. C. Bhatt, and C. M. Sunta, *J. Lumin*. **130**, 1216 (2010).

[37] A. J. J. Bos, *Rad. Meas.* **41**, S45 (2007).

[38] E. Borchi, M. Bruzzi, S. Pirollo, and S. Sciortino, *J. Phys. D: Appl. Phys.* **31**, L93 (1998).

[39] N. S. Yüksek, N. M. Gasanly, and H. Özkan, *Semicond. Sci. Technol.* **18**, 834 (2003).

[40] T. A. T. Cowell and J. Woods, *Brit. J. Appl. Phys.* **18**, 1047 (1967).

[41] C. Manfredotti, R. Murri, A. Quirini, and L. Vasanelli, *Phys. Stat. Sol. (a)* **38**, 685 (1976).

[42] N. F. Mott and E. A. Davis, *Electronic Processes in Non-Crystalline Materials*, Clarendon Press, Oxford (1979).

[43] A. Serpi, *J. Phys. D: Appl. Phys*. **9**, 1881 (1976).

[44] N. S. Yuksek, N. M. Gasanly, and H. Ozkan, Progress in Condensed Matter Physics *"Thermally Stimulated Current Observation of Trapping Centers in Layered Thallium Dichalcogenide Semiconductors"*, Nova Science Publishers, Inc. (2004).

[45] T. Pisarkiewicz, *Opt. Elect. Rev.* **12**, 33 (2004).

[46] N. M. Gasanly, H. Özkan, and N. A. P. Mogaddam, *Semicond. Sci. Technol.* **21**, 1250 (2006).

[47] J. R. Drabble and H. J. Goldsmid, *Thermal Conduction in Semiconductors* (Pergamon, Oxford, 1961), p. 191.

[48] A. F. Qasrawi and N. M. Gasanly, *Cryst. Res. Technol*. **41**, 174 (2005).

[49] S. H. Wemple and M. DiDomenico, *Phys. Rev*. B **3**, 1338 (1971).

[50] F. Yakuphanoglu, A. Cukurovali, and I. Yilmaz, *Physica B* **351**, 53 (2004).

[51] F. Yakuphanoglu, A. Cukurovali, and I. Yılmaz, *Physica B* **353**, 210 (2004).

[52] E. Marguez, P. Nagels, J. M. Gonzalez-Leal, A. M. Bernal-Oliva, E. Sleecks, and R. Callaerts, *Vacuum* **52**, 55 (1999).

[53] E. Marguez, A. M. Bernal-Oliva, L. M. Gonzalez-Leal, R. Pricto-Alcon, A. Ledesma, R. Jimenez-Garay, and I. Martil, *Mater. Chem. Phys.* **60**, 231 (1999).

[54] A. Bosacchi, B. Bosacchi, S. Franchia, and L. Hernandez, *Sol. Stat. Commun.* **13**, 1805 (1973).

[55] A. Anedda, M. B. Casu, A. Serpi, I. I. Burlakov, I. M. Tiginyanu, and V. V. Ursaki, *J. Phys. Chem. Solids* **58**, 325 (1997).

[56] S. N. Singh, B. A. Sharma, and A. N. Singh, *Int. J. Mod. Phys. B* **20**, 3307 (2006).

[57] A. F. Qasrawi and N. M. Gasanly, *Cryst. Res. Technol.* **41**, 174 (2006).